

Structural Studies of β -Turn-Containing Peptide Catalysts for Atroposelective Quinazolinone Bromination

Anthony J. Metrano,[†] Nadia C. Abascal,[†]
Brandon Q. Mercado, Eric K. Paulson, and Scott J. Miller*

Department of Chemistry, Yale University, New Haven, CT 06520-8107, United States

*E-mail: scott.miller@yale.edu

[†] A.J.M. and N.C.A. contributed equally.

Electronic Supplementary Information

Table of Contents

I. General Information.....	S2
II. Solution Phase Peptide Synthesis and Characterization	S4
III. Synthesis and Characterization of Quinazolin-4(3 <i>H</i>)-one 1	S15
IV. Bromination Procedures and Characterization of Tribromide 2	S16
V. Solution-Phase NMR Studies of 3 and 4I	S20
VI. Crystallographic Information	S32
VII. References.....	S36

I. General Information

Room temperature (rt) is defined as 21–23 °C. All reagents were purchased from commercial suppliers and used without further purification, unless otherwise noted. In particular, *N*-bromosuccinimide (NBS) was recrystallized from water, dried thoroughly *in vacuo*, and stored in a vial shielded from light at 0 °C. Methylene chloride (CH₂Cl₂), and toluene (PhMe) were obtained from a Seca Solvent System by GlassContour, in which the solvent was dried over alumina and dispensed under an atmosphere of Ar. All other solvents were purchased from commercial suppliers and used without further purification.

Routine ¹H-NMR spectra were recorded on Agilent 500 MHz spectrometers at ambient temperature. NMR solvents, *d*-chloroform, *d*₆-dimethylsulfoxide, *d*₆-benzene, and *d*₄-methanol were purchased from Cambridge Isotope Laboratories and used without further purification. *d*-Chloroform was stored at ambient temperature over 4 Å molecular sieves, and fresh *d*₄-methanol and *d*₆-benzene ampules were used immediately after opening. Spectra were processed with MestReNova 10.0.2 using the automatic phasing and Bernstein third order polynomial baseline correction capabilities. Splitting was determined using the automatic multiplet analysis function with intervention as necessary. Spectral data are reported as follows: chemical shift (multiplicity [singlet (s), doublet (d), triplet (t), quartet (q), pentet (p), multiplet (m), doublet of doublets (dd), doublet of doublet of doublets (ddd), doublet of triplet of doublets (dtd), doublet of triplets (dt), triplet of doublets (td), etc.], coupling constant, integration). Chemical shifts are reported in ppm (δ), and coupling constants are reported in Hz. ¹H-Resonances are referenced to solvent residual peaks for CDCl₃ (7.26 ppm), DMSO-*d*₆ (2.50 ppm), C₆D₆ (7.16 ppm), or CD₃OD (3.31 ppm).¹ Routine ¹³C-NMR spectra were recorded on Agilent 500 MHz spectrometers with protons fully decoupled. ¹³C-Resonances are reported in ppm relative to solvent residual peaks for CDCl₃ (77.2 ppm), DMSO-*d*₆ (39.5 ppm), C₆D₆ (128.1 ppm), or CD₃OD (49.0 ppm).¹

Infrared spectra were recorded on a Nicolet 6700 ATR/FT-IR spectrometer, and ν_{\max} are partially reported in cm⁻¹. Samples for high-resolution liquid chromatography-mass spectrometry (HRMS) were submitted to the Mass Spectrometry Laboratory at the University of Illinois at Urbana-Champaign. Data was acquired on a Waters Synapt G2-Si instrument equipped with an ESI detector. For crude analysis, ultra high-performance liquid chromatography-mass spectrometry (UPLC/MS) was performed on a Waters Acquity UPLC/MS instrument equipped with a reverse-phase BEH C18 column (1.7 μm particle size, 2.1 x 50 mm), a dual atmospheric pressure chemical ionization (API)/electrospray ionization (ESI) mass spectrometry detector, and a photodiode array detector.

Analytical thin-layer chromatography (TLC) was performed using 60 Å Silica Gel F₂₅₄ pre-coated plates (0.25 mm thickness). TLC plates were visualized by irradiation with a UV lamp. R_f values are reported. Normal-phase flash chromatography was performed using a Biotage Isolera One purification system equipped with a 10, 25, or 50 g SNAP Ultra (HP Sphere, 25 mm silica) cartridge and an appropriate EtOAc/hexanes linear gradient in the mobile phase. Reverse-phase column chromatography was performed using a Biotage Isolera One purification

system equipped with a 60 or 120 g SNAP-C18 column and an appropriate MeOH/H₂O linear gradient in the mobile phase.

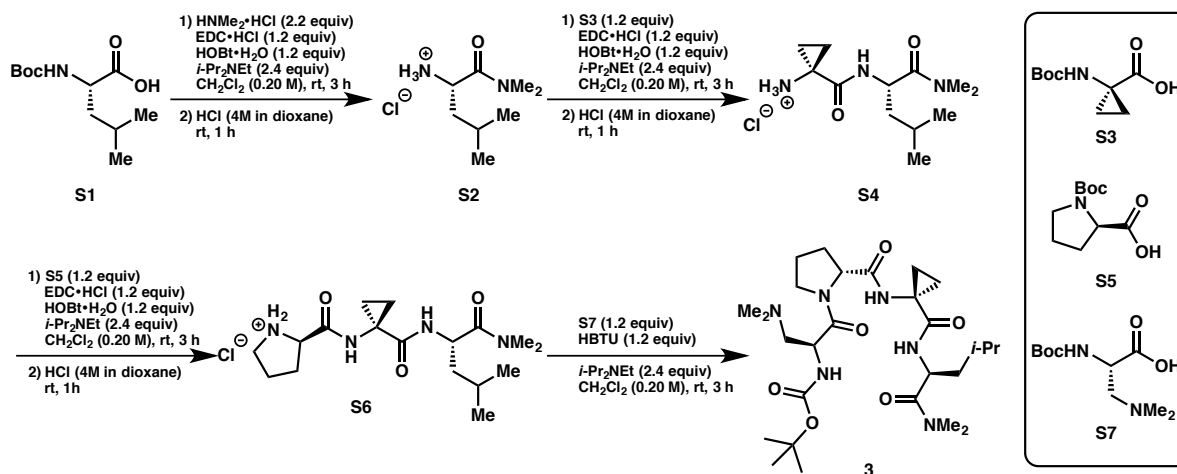
Optical rotations were recorded on a Perkin-Elmer Polarimeter 341 at the sodium D-line (589 nm) using a cell of 1 dm path length. Measurements were recorded at 20 °C. Concentration values are reported in units of g/100 mL. Normal-phase high-performance liquid chromatography (HPLC) was performed using an Agilent 1100 series instrument equipped with a diode array detector and columns (chiral supports) from Daicel Chemical Industries (Chiralcel OJ-H).

II. Solution Phase Peptide Synthesis and Characterization

A. General Remarks

The solution phase peptide synthesis of catalysts **3**, **4a–x**, and **S11–18** was accomplished using the *N*-*tert*-butoxycarbonyl (Boc) protecting group strategy.² Boc-L-β-Dimethylaminoalanine (**S7**, Boc-Dmaa-OH) was synthesized according to a literature procedure.³ All other amino acid residues and coupling reagents were purchased from commercial suppliers. Once synthesized, peptides were stored at 0 °C to prevent epimerization and other adverse side-reactivity.

B. Synthesis and Characterization of Dimethylamide-Containing Peptide **3**



Installation of C-Terminal Protecting Group: Boc-Leu-OH·H₂O (**S1**, 499 mg, 2.00 mmol), dimethylamine hydrochloride (359 mg, 4.40 mmol), and HOBT·H₂O (368 mg, 2.40 mmol) were added to a round bottom flask equipped with a magnetic stir bar. The solid mixture was dissolved in CH₂Cl₂ (10 mL, 0.20 M w.r.t. **S1**), and EDC·HCl (460 mg, 2.40 mmol) was added. The resulting solution was allowed to stir at rt as *i*-Pr₂NEt (0.84 mL, 4.80 mmol) was added slowly, causing the cloudy solution to clarify. The pale yellow reaction solution was allowed to stir at rt for about 2 h, after which the solution was poured into a separatory funnel, diluted to 30 mL with additional CH₂Cl₂, and washed with approximately 25 mL of 10% aqueous (w/v) citric acid. The organic layer was separated and subsequently washed with 25 mL each of saturated aqueous NaHCO₃ and brine. The organics were dried over anhydrous Na₂SO₄, filtered, and concentrated *in vacuo* to provide a clear, pale yellow oil (517 mg, > 99% crude yield). The identity of Boc-Leu-NMe₂ was confirmed by UPLC/MS. **MS:** Exact mass calculated for [C₁₃H₂₆N₂O₃ + H]⁺ requires *m/z* = 259.2. Found 259.2 (ESI+).

Deprotection 1: Crude Boc-Leu-NMe₂ was then treated with 6 mL of 4.0 M HCl in 1,4-dioxane to cleave the Boc group. The resulting pale yellow solution was allowed to stir at rt for 1 h before HCl and 1,4-dioxane were removed *in vacuo*. Residual 1,4-dioxane was removed by co-

evaporation with CH₂Cl₂ to provide 389 mg (> 99% crude yield) of **S2** as a foam, which was dried thoroughly under reduced pressure before being carried forward to the next coupling step.

Peptide Coupling 1: To a flask containing H-Leu-NMe₂•HCl (**S2**, 389 mg, 2.00 mmol) was added Boc-Acpc-OH (**S3**, 483 mg, 2.20 mmol), HOBt•H₂O (368 mg, 2.40 mmol), and a magnetic stir bar. The solid mixture was dissolved in dry CH₂Cl₂ (10.0 mL, 0.20 M w.r.t. **S2**), and EDC•HCl (460 mg, 2.40 mmol) was then added. The resulting solution was allowed to stir at rt as *i*-Pr₂NEt (0.84 mL, 4.80 mmol) was added slowly. The deep yellow reaction solution was allowed to stir at rt for 2 h, after which the solution was poured into a separatory funnel, diluted to 30 mL with additional CH₂Cl₂, and washed with 25 mL of 10% aqueous (w/v) citric acid. The organic layer was separated and subsequently washed with 25 mL each of saturated aqueous NaHCO₃ and brine. The organics were dried over anhydrous Na₂SO₄, filtered, and concentrated *in vacuo* to provide a white foam (739 mg, > 99% crude yield). The identity of Boc-Acpc-Leu-NMe₂ was confirmed by UPLC-MS. **MS:** Exact mass calculated for [C₁₇H₃₁N₃O₄ + H]⁺ requires *m/z* = 342.2. Found 342.3 (ESI+).

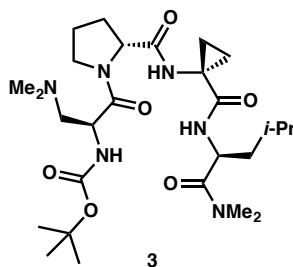
Deprotection 2: Deprotection of the crude dipeptide Boc-Acpc-Leu-NMe₂ was accomplished in the same manner as described in Deprotection 1 (*vide supra*) to provide **S4** (556 mg, 2.00 mmol) as a white foam.

Peptide Coupling 2: To a flask containing H-Acpc-Leu-NMe₂•HCl (**S4**, 556 mg, 2.00 mmol) was added Boc-D-Pro-OH (**S3**, 517 mg, 2.20 mmol), HOBt•H₂O (368 mg, 2.40 mmol), and a magnetic stir bar. The solid mixture was dissolved in dry CH₂Cl₂ (10.0 mL, 0.20 M w.r.t. **S4**), and EDC•HCl (460 mg, 2.40 mmol) was then added. The resulting solution was allowed to stir at rt as *i*-Pr₂NEt (0.84 mL, 4.80 mmol) was added slowly. The deep yellow reaction solution was allowed to stir at rt for 2 h, after which the solution was poured into a separatory funnel, diluted to 30 mL with additional CH₂Cl₂, and washed with 25 mL of 10% aqueous (w/v) citric acid. The organic layer was separated and subsequently washed with 25 mL each of saturated aqueous NaHCO₃ and brine. The organics were dried over anhydrous Na₂SO₄, filtered, and concentrated *in vacuo* to provide a white foam (873 mg, > 99% crude yield). The identity of Boc-D-Pro-Acpc-Leu-NMe₂ was confirmed by UPLC-MS. **MS:** Exact mass calculated for [C₂₂H₃₈N₄O₅ + H]⁺ requires *m/z* = 439.3. Found 439.4 (ESI+).

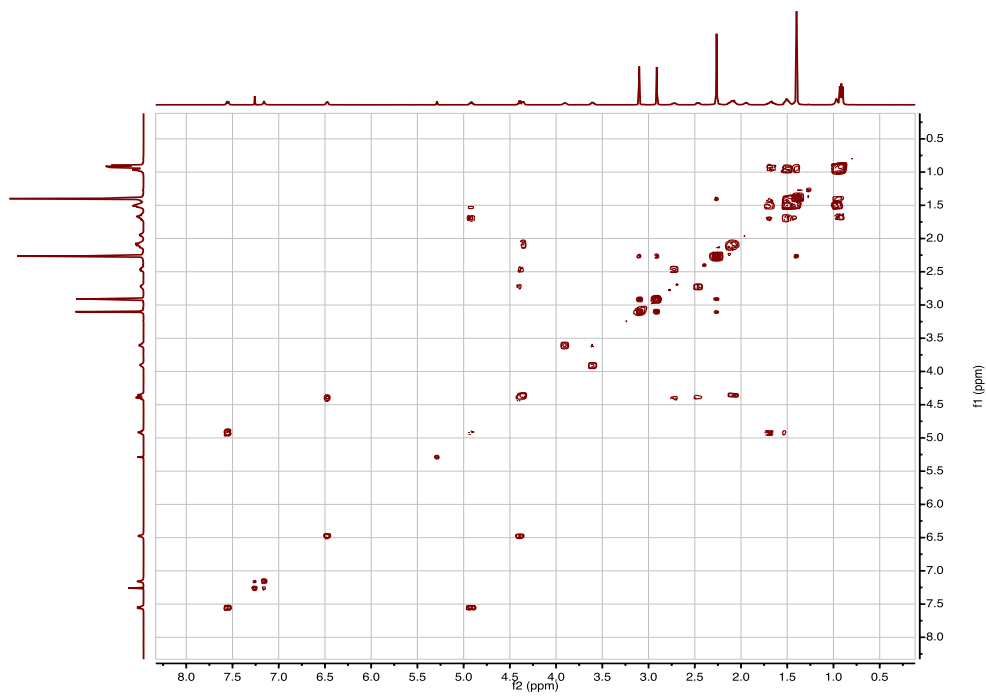
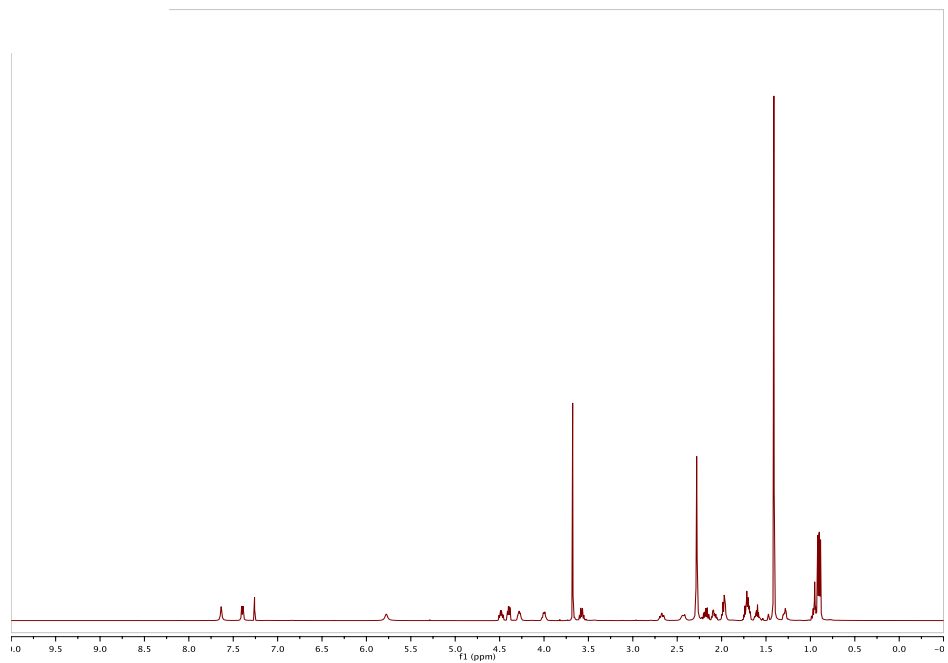
Deprotection 3: Deprotection of the crude tripeptide Boc-D-Pro-Acpc-Leu-NMe₂ was accomplished in the same manner as described in Deprotection 1 (*vide supra*) to provide **S6** (750 mg, 2.00 mmol) as an off-white foam.

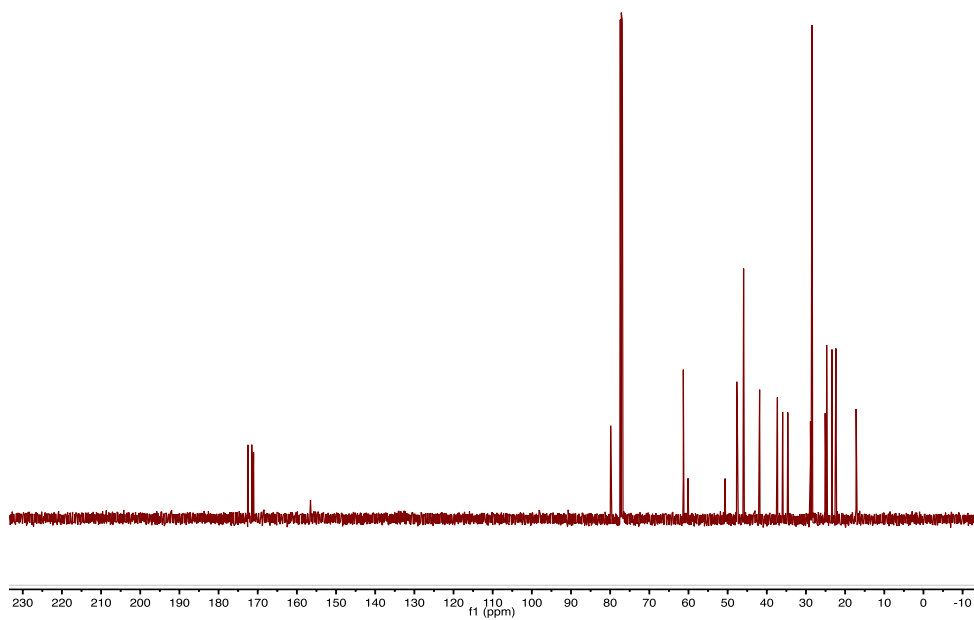
Peptide Coupling 3: To a flask containing H-D-Pro-Acpc-Leu-NMe₂•HCl (**S6**, 750 mg, 2.00 mmol) was added Boc-Dmaa-OH (**S7**, 511 mg, 2.20 mmol) and a magnetic stir bar. The solid mixture was dissolved in CH₂Cl₂ (10.0 mL, 0.20 M w.r.t. **S6**), and HBTU (910 mg, 2.40 mmol) was then added to the stirring solution at rt. Next, *i*-Pr₂NEt (0.84 mL, 4.80 mmol) was added slowly. The deep yellow/brown reaction solution was allowed to stir at rt for 8 h, after which the solution was poured into a separatory funnel, diluted to 30 mL with additional CH₂Cl₂, and washed twice with about 25 mL of saturated aqueous NaHCO₃. The organic layer was

separated and subsequently washed with 20 mL of brine. The organics were dried over anhydrous Na₂SO₄, filtered, and concentrated *in vacuo* to provide a deep yellow oil. The crude product was loaded onto a Biotage Isolera One purification system for reverse-phase column chromatography (120 g column, 30-100% MeOH/H₂O over 16 column volumes with 3 column volume pre- and post-run equilibrations, 45 mLmin⁻¹ flow, collection λ = 210 nm, monitored λ = 254 nm, 16 x 150 mm test tubes with 20 mL fractions). Fractions were pooled, concentrated *in vacuo*, and dried thrice azeotropically with CH₂Cl₂ to provide Boc-Dmaa-D-Pro-Acpc-Leu-NMe₂ (**3**, 667 mg, 60% yield) as a white foam.

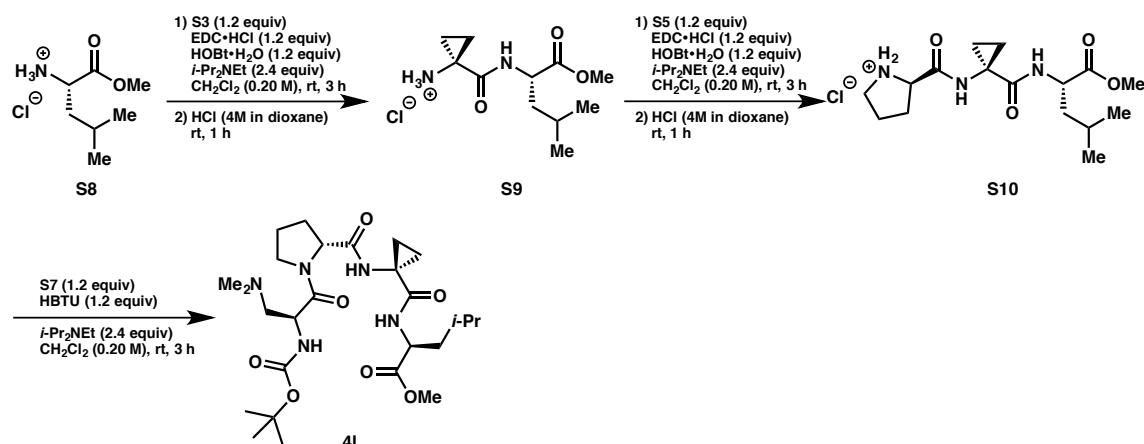


Boc-Dmaa-D-Pro-Acpc-Leu-NMe₂ (3): White foamy solid, 60% overall yield from **S1**. **IR** (FT-ATR, cm⁻¹): 3301, 2969, 2873, 1627, 1519, 1445, 1245, 1165, 1010. **¹H-NMR** (500 MHz, CDCl₃): δ 7.55 (d, *J* = 8.5 Hz, 1H), 7.16 (s, 1H), 6.48 (d, *J* = 6.3 Hz, 1H), 4.92 (td, *J* = 8.6, 5.1 Hz, 1H), 4.39 (q, *J* = 7.1 Hz, 1H), 4.36 (dd, *J* = 7.6, 4.1 Hz, 1H), 4.03–3.91 (m, 1H), 3.60 (dt, *J* = 9.9, 6.8 Hz, 1H), 3.10 (s, 3H), 2.91 (s, 3H), 2.72 (dd, *J* = 12.3, 7.6 Hz, 1H), 2.46 (dd, *J* = 12.3, 7.2 Hz, 1H), 2.26 (s, 6H), 2.16–2.10 (m, 3H), 1.99–1.90 (m, 1H), 1.73–1.61 (m, 2H), 1.55–1.46 (m, 3H), 1.40 (s, 9H), 0.97 (dq, *J* = 6.3, 3.2 Hz, 2H), 0.92 (dd, *J* = 9.4, 6.4 Hz, 6H). **¹³C-NMR** (125 MHz, CDCl₃): δ 172.5, 172.3, 171.5, 171.1, 156.5, 79.9, 76.9, 61.3, 60.1, 50.6, 47.7, 47.5, 45.9, 41.8, 37.3, 36.0, 34.6, 28.9, 28.5, 25.1, 24.7, 23.4, 22.4, 17.2, 17.1. **HRMS:** Exact mass calculated for [C₂₇H₄₈N₆O₆ + H]⁺ requires *m/z* = 553.3714. Found 553.3709 (ESI+). **Optical:** [α]_D²⁰ = +40.2 (*c* = 1.0, CH₂Cl₂).





C. Synthesis and Characterization of Methyl Ester-Containing Peptide 4I



Peptide Coupling 1: To a flask containing H-Leu-OMe•HCl (**S8**, 362 mg, 2.00 mmol) was added Boc-Acpc-OH (**S3**, 483 mg, 2.40 mmol), HOBT•H₂O (368 mg, 2.40 mmol), and a magnetic stir bar. The solid mixture was dissolved in dry CH₂Cl₂ (10.0 mL, 0.20 M w.r.t. **S8**), and EDC•HCl (460 mg, 2.40 mmol) was then added. The resulting solution was allowed to stir at rt as *i*-Pr₂NEt (0.84 mL, 4.80 mmol) was added slowly. The clear, colorless reaction solution was allowed to stir at rt for overnight, after which the solution was poured into a separatory funnel, diluted to 30 mL with additional CH₂Cl₂, and washed with 25 mL of 10% aqueous (w/v) citric acid. The organic layer was separated and subsequently washed with 25 mL each of saturated aqueous NaHCO₃ and brine. The organics were dried over anhydrous Na₂SO₄, filtered, and concentrated *in vacuo* to provide an off-white waxy solid (772 mg, > 99% crude yield). The identity of Boc-Acpc-Leu-OMe was confirmed by UPLC-MS. **MS:** Exact mass calculated for [C₁₆H₂₈N₂O₅ + H]⁺ requires *m/z* = 329.2. Found 329.3 (ESI+).

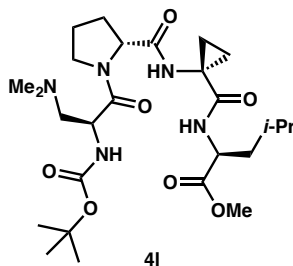
Deprotection 1: Crude Boc-Acpc-Leu-OMe was then treated with 6 mL of 4.0 M HCl in 1,4-dioxane to cleave the Boc group. The resulting pale yellow solution was allowed to stir at rt for 1 h, before HCl and 1,4-dioxane were removed *in vacuo*. Residual 1,4-dioxane was removed by co-evaporation with CH₂Cl₂ to provide 530 mg (> 99% crude yield) of **S9** as a foam, which was dried thoroughly under reduced pressure before being carried forward to the next coupling step.

Peptide Coupling 2: To a flask containing H-Acpc-Leu-OMe•HCl (**S9**, 530 mg, 2.00 mmol) was added Boc-D-Pro-OH (**S5**, 517 mg, 2.20 mmol), HOBT•H₂O (368 mg, 2.40 mmol), and a magnetic stir bar. The solid mixture was dissolved in dry CH₂Cl₂ (10.0 mL, 0.20 M w.r.t. **S9**), and EDC•HCl (460 mg, 2.40 mmol) was then added. The resulting solution was allowed to stir at rt as *i*-Pr₂NEt (0.84 mL, 4.80 mmol) was added slowly. The clear, pale yellow reaction solution was allowed to stir at rt for 3 h, after which the solution was poured into a separatory funnel, diluted to 30 mL with additional CH₂Cl₂, and washed with 25 mL of 10% aqueous (w/v) citric acid. The organic layer was separated and subsequently washed with 25 mL each of saturated aqueous NaHCO₃ and brine. The organics were dried over anhydrous Na₂SO₄, filtered, and concentrated *in vacuo* to provide a white foam (851 mg, 1.86 mmol, 93% crude yield). The

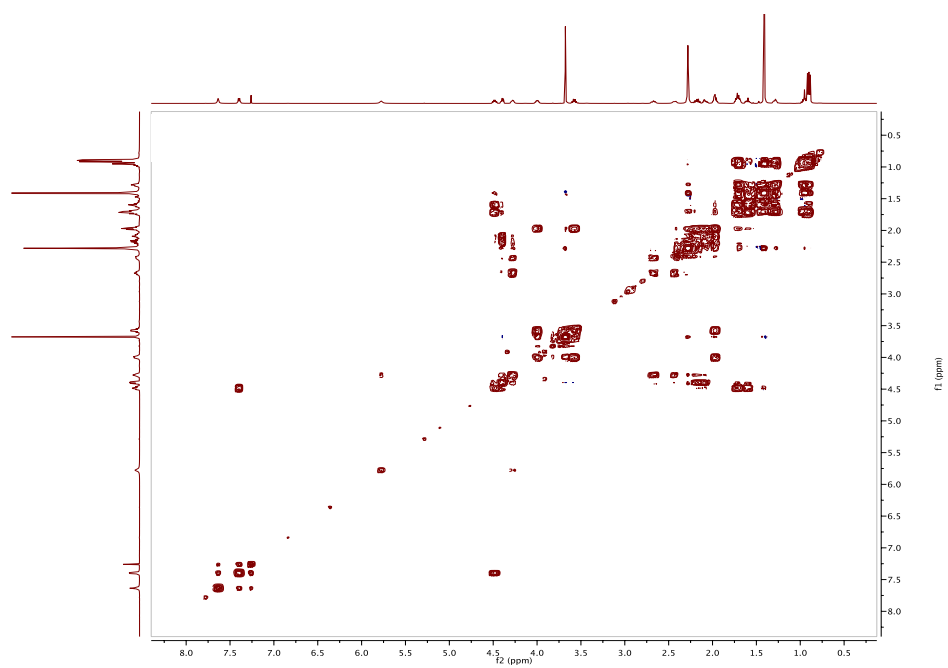
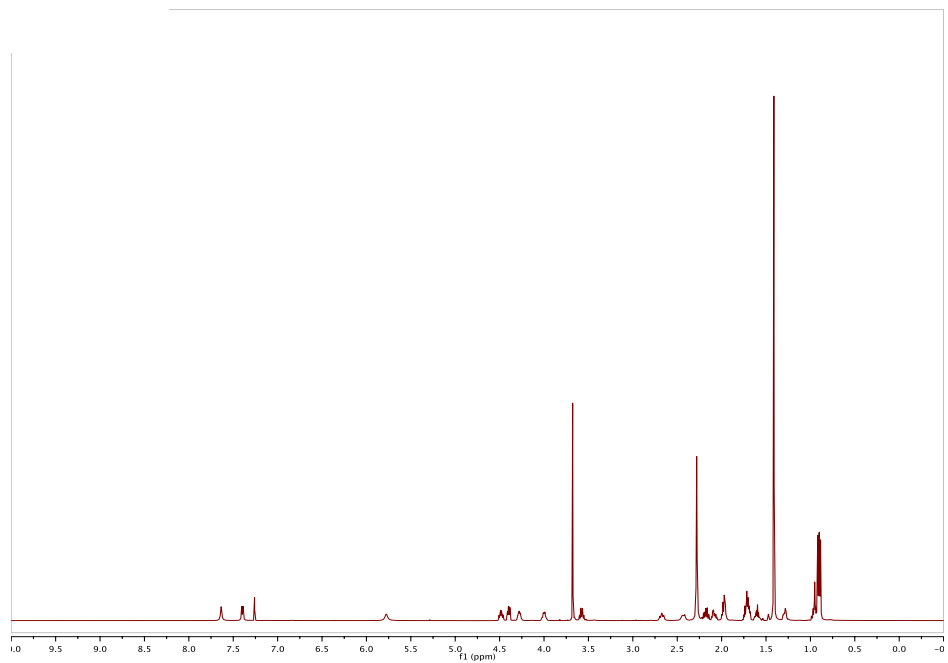
identity of Boc-D-Pro-Acpc-Leu-OMe was confirmed by UPLC-MS. **MS**: Exact mass calculated for $[C_{21}H_{35}N_3O_6 + H]^+$ requires $m/z = 426.3$. Found 426.4 (ESI+).

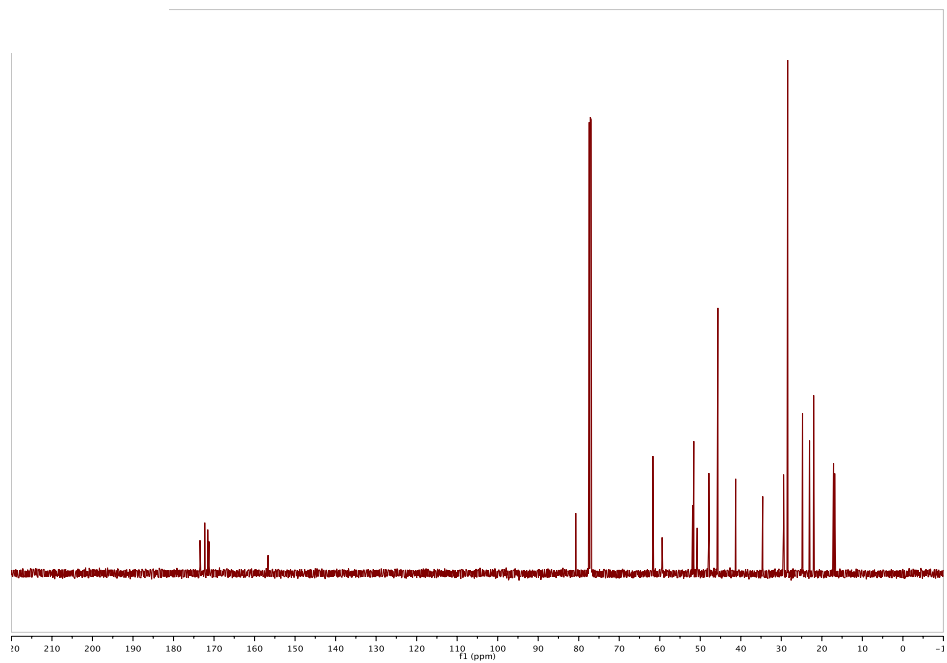
Deprotection 2: Deprotection of the crude tripeptide Boc-D-Pro-Acpc-Leu-OMe was accomplished in the same manner as described in Deprotection 1 (*vide supra*) to provide 672 mg of **S10** (1.86 mmol, > 99% crude yield) as an off-white foam.

Peptide Coupling 3: To a flask containing H-D-Pro-Acpc-Leu-OMe•HCl (**S10**, 672 mg, 1.86 mmol) was added Boc-Dmaa-OH (**S76**, 518 mg, 2.23 mmol) and a magnetic stir bar. The solid mixture was dissolved in CH_2Cl_2 (9.3 mL, 0.20 M w.r.t. **S10**), and HBTU (846 mg, 2.23 mmol) was then added to the stirring solution at rt. Next, *i*-Pr₂NEt (0.78 mL, 4.46 mmol) was added slowly. The deep yellow reaction solution was allowed to stir at rt for 8 h, after which the solution was poured into a separatory funnel, diluted to 30 mL with additional CH_2Cl_2 , and washed twice with about 25 mL of saturated aqueous $NaHCO_3$. The organic layer was separated and subsequently washed with 20 mL of brine. The organics were dried over anhydrous Na_2SO_4 , filtered, and concentrated *in vacuo* to provide a deep yellow oil. The crude product was loaded onto a Biotage Isolera One purification system for reverse-phase column chromatography (120 g column, 30-100% MeOH/ H_2O over 16 column volumes with 3 column volume pre- and post-run equilibrations, 45 mLmin⁻¹ flow, collection $\lambda = 210$ nm, monitored $\lambda = 254$ nm, 16 x 150 mm test tubes with 20 mL fractions). Fractions were pooled, concentrated *in vacuo*, and dried thrice azeotropically with CH_2Cl_2 to provide Boc-Dmaa-D-Pro-Acpc-Leu-OMe (**4I**, 759 mg, 76% yield) as a white foam.

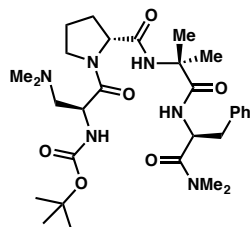


Boc-Dmaa-D-Pro-Acpc-Leu-OMe (4I): White foamy solid, 76% overall yield from **S8**. **IR** (FT-ATR, cm^{-1}): 3322, 2956, 1744, 1669, 1644, 1539, 1506, 1442, 1367, 1254, 1169, 1023. **¹H-NMR** (600 MHz, $CDCl_3$): δ 7.64 (s, 1H), 7.40 (d, $J = 7.7$ Hz, 1H), 5.78 (s, 1H), 4.48 (ddd, $J = 9.0, 7.6, 5.3$ Hz, 1H), 4.40 (dd, $J = 8.5, 4.3$ Hz, 1H), 4.34–4.22 (m, 1H), 4.00 (dt, $J = 9.9, 6.3$ Hz, 1H), 3.68 (s, 3H), 3.58 (dt, $J = 9.7, 7.5$ Hz, 1H), 2.67 (t, $J = 11.1$ Hz, 1H), 2.48–2.35 (m, 1H), 2.28 (s, 6H), 2.18 (dq, $J = 12.9, 8.2$ Hz, 1H), 2.13–2.02 (m, 1H), 2.02–1.89 (m, 2H), 1.71 (ddt, $J = 13.8, 6.7, 5.0$ Hz, 3H), 1.60 (tt, $J = 9.9, 5.3$ Hz, 1H), 1.41 (s, 9H), 1.31–1.27 (m, 1H), 1.02 - 0.93 (m, 1H), 0.90 (dd, $J = 9.6, 6.2$ Hz, 6H). **¹³C-NMR** (125 MHz, $CDCl_3$): δ 173.5, 172.3, 171.5, 171.2, 156.7, 80.7, 77.4, 77.2, 76.9, 61.7, 59.4, 51.9, 51.6, 50.8, 47.9, 45.7, 41.3, 34.6, 29.5, 28.5, 28.4, 24.8, 24.8, 23.0, 22.0, 17.1, 16.8. **HRMS**: Exact mass calculated for $[C_{26}H_{45}N_5O_7 + H]^+$ requires $m/z = 540.3397$. Found 540.3394 (ESI+). **Optical**: $[\alpha]_D^{20} = -2.96$ ($c = 1.0, CHCl_3$).

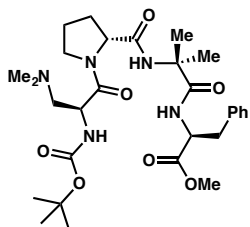




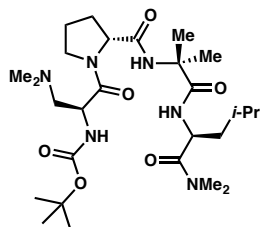
D. HRMS Data for Peptide Catalysts 4a–k, 4m–x, and S11–18



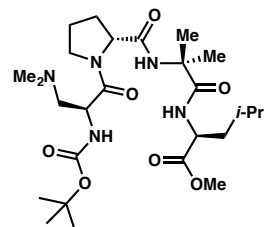
4a
Calculated $[C_{30}H_{48}N_6O_6 + H]^+$
requires $m/z = 589.3714$.
Found 589.3707.



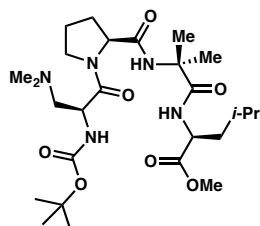
4b
Calculated $[C_{29}H_{45}N_6O_7 + H]^+$
requires $m/z = 576.3397$.
Found 576.3389.



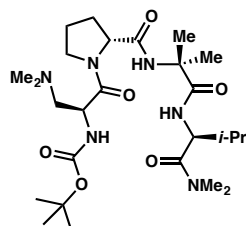
4c
Calculated $[C_{27}H_{40}N_6O_6 + H]^+$
requires $m/z = 555.3870$.
Found 555.3869.



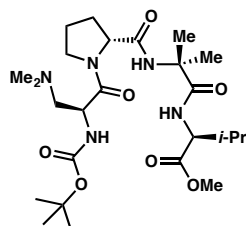
4d
Calculated $[C_{26}H_{37}N_6O_7 + H]^+$
requires $m/z = 542.3554$.
Found 542.3543.



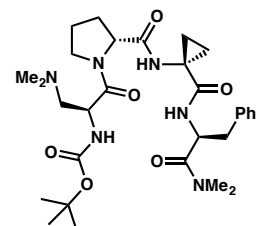
4e
Calculated $[C_{26}H_{47}N_5O_7 + H]^+$
requires $m/z = 542.3554$.
Found 542.3555.



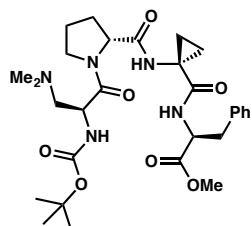
4f
Calculated $[C_{26}H_{46}N_5O_6 + H]^+$
requires $m/z = 541.3714$.
Found 541.3718.



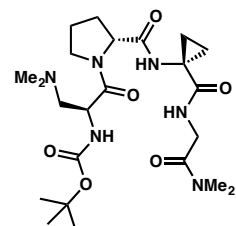
4g
Calculated $[C_{25}H_{45}N_5O_7 + H]^+$
requires $m/z = 528.3397$.
Found 528.3398.



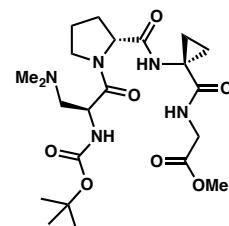
4h
Calculated $[C_{30}H_{46}N_6O_6 + H]^+$
requires $m/z = 587.3557$.
Found 587.3549.



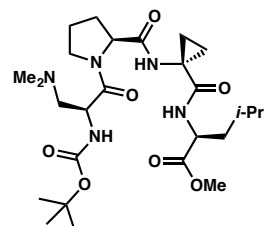
4i
Calculated $[C_{29}H_{43}N_5O_7 + H]^+$
requires $m/z = 574.3241$.
Found 574.3235.



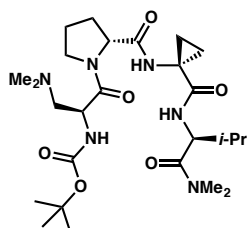
4j
Calculated $[C_{23}H_{40}N_6O_6 + H]^+$
requires $m/z = 497.3088$.
Found 497.3081.



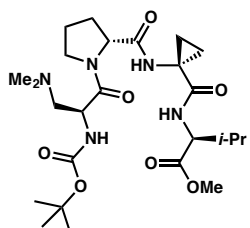
4k
Calculated $[C_{22}H_{37}N_5O_7 + H]^+$
requires $m/z = 484.2771$.
Found 484.2768.



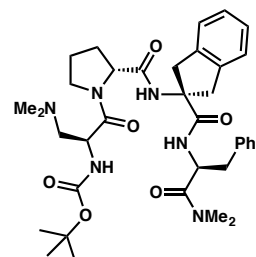
4m
Calculated $[C_{26}H_{45}N_5O_7 + H]^+$
requires $m/z = 540.3397$.
Found 540.3387.



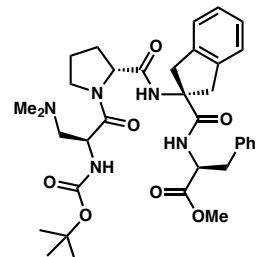
4n
Calculated $[C_{25}H_{46}N_6O_6 + H]^+$
requires $m/z = 539.3557$.
Found 539.3555.



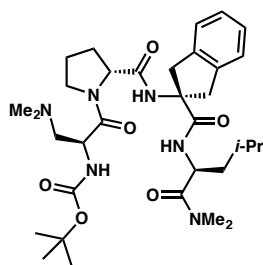
4o
Calculated $[C_{25}H_{43}N_5O_7 + H]^+$
requires $m/z = 526.3241$.
Found 526.3240.



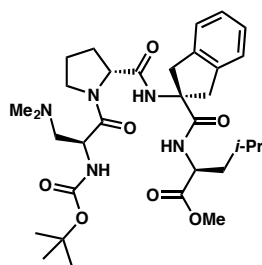
4p
Calculated $[C_{36}H_{50}N_6O_6 + H]^+$
requires $m/z = 663.3870$.
Found 663.3863.



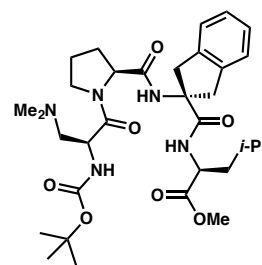
4q
Calculated $[C_{35}H_{47}N_5O_7 + H]^+$
requires $m/z = 650.3554$.
Found 650.3557.



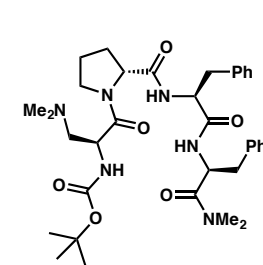
4r
Calculated $[C_{33}H_{52}N_6O_6 + H]^+$
requires $m/z = 629.4027$.
Found 629.4022.



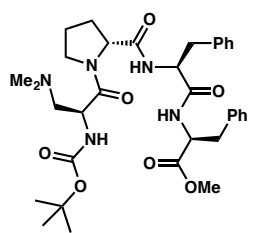
4s
Calculated $[C_{32}H_{49}N_5O_7 + H]^+$
requires $m/z = 616.3710$.
Found 616.3706.



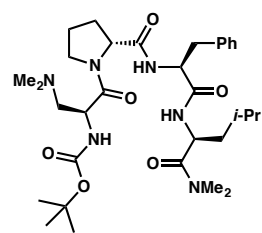
4t
Calculated $[C_{32}H_{49}N_5O_7 + H]^+$
requires $m/z = 616.3710$.
Found 616.3702.



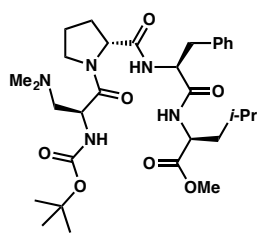
4u
Calculated $[C_{35}H_{50}N_6O_6 + H]^+$
requires $m/z = 651.3870$.
Found 651.3858.



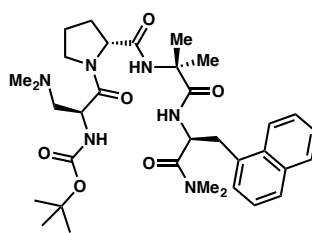
4v
Calculated $[C_{34}H_{47}N_5O_7 + H]^+$
requires $m/z = 638.3554$.
Found 638.3544.



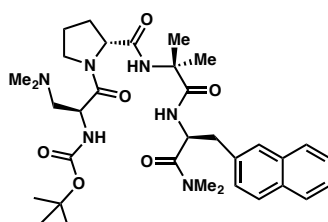
4w
Calculated $[C_{32}H_{52}N_6O_6 + H]^+$
requires $m/z = 617.4027$.
Found 617.4023.



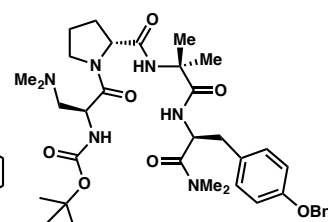
4x
Calculated $[C_{31}H_{49}N_5O_7 + H]^+$
requires $m/z = 604.3710$.
Found 604.3716.



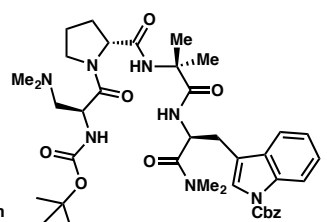
S11
Calculated $[C_{34}H_{50}N_6O_6 + H]^+$
requires $m/z = 639.3870$.
Found 639.3865.



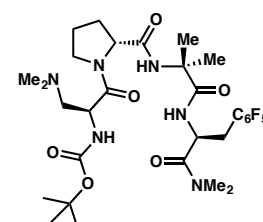
S12
Calculated $[C_{34}H_{50}N_6O_6 + H]^+$
requires $m/z = 639.3870$.
Found 639.3861.



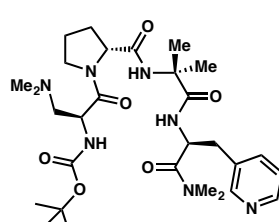
S13
Calculated $[C_{37}H_{54}N_6O_7 + H]^+$
requires $m/z = 695.4132$.
Found 695.4125.



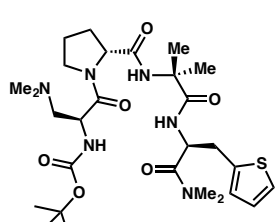
S14
Calculated $[C_{40}H_{59}N_7O_8 + H]^+$
requires $m/z = 762.4190$.
Found 762.4184.



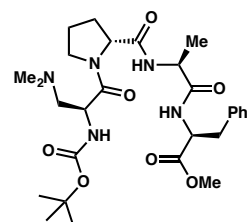
S15
Calculated $[C_{30}H_{43}F_5N_6O_6 + H]^+$
requires $m/z = 679.3242$.
Found 679.3240.



S16
Calculated $[C_{29}H_{47}N_7O_6 + H]^+$
requires $m/z = 590.3666$.
Found 590.3658.

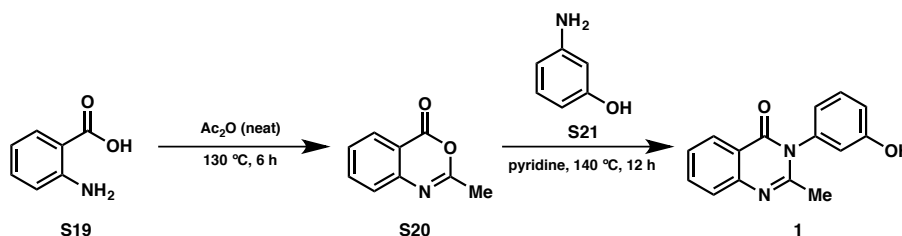


S17
Calculated $[C_{29}H_{46}N_6O_6S + H]^+$
requires $m/z = 595.3278$.
Found 595.3278.



S18
Calculated $[C_{28}H_{44}N_5O_7 + H]^+$
requires $m/z = 562.3241$.
Found 562.3237.

III. Synthesis and Characterization of Quinazolin-4(3*H*)-one **1**

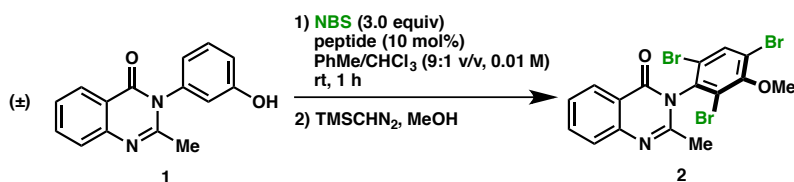


2-Methyl-4*H*-benzo-[d][1,3]oxazin-4-one (S20):⁴ Anthranilic acid (**S19**, 8.228 g, 60.0 mmol) was added to an oven-dried 40 mL sealed tube (thick-walled) equipped with a magnetic stir bar. The off-white solid was suspended in acetic anhydride (36 mL, 381 mmol), and the vessel was purged with nitrogen, sealed tightly, and submerged into an oil bath at $130\text{ }^\circ\text{C}$. The cloudy suspension quickly became a clear, deep yellow solution, which was allowed to stir at $130\text{ }^\circ\text{C}$ for 6 h. The reaction solution was allowed to cool to room temperature, and the contents of the sealed tube were transferred to a round bottom flask washing with copious PhMe. Removal of solvent under reduced pressure yielded benzoxazinone **S20** (9.503 g, 98% yield) which was used without further purification.

3-(3-Hydroxyphenyl)-2-methylquinazolin-4(3*H*)-one (1):⁵ Benzoxazinone **S20** (2.991 g, 18.6 mmol) and *m*-aminophenol (**S21**, 2.430 g, 22.3 mmol) were added to an oven-dried 40 mL sealed tube (thick-walled) equipped with a magnetic stir bar. The solid mixture was dissolved in pyridine (16.7 mL, 1.2 M w.r.t. **S20**). The vessel was purged with nitrogen, sealed tightly, and submerged in an oil bath at $145\text{ }^\circ\text{C}$. The cloudy, deep red suspension began to clarify upon heating. The deep red solution was allowed to stir for 12 h at $145\text{ }^\circ\text{C}$, after which the vessel was cooled to room temperature. The contents of the sealed tube were transferred to a round bottom flask, washing with copious PhMe, and the solvent was removed under reduced pressure. The crude product was purified by automated flash chromatography using a gradient of 10–100% EtOAc/hexanes. Fractions were pooled and concentrated *in vacuo* to provide a pale yellow solid, which was suspended in hot CH_2Cl_2 and vacuum filtered to remove insoluble side-products. The filtrate was allowed to cool to $0\text{ }^\circ\text{C}$, precipitating 2.563 g (61% yield) of pure **1** as a white solid. **TLC:** $R_f = 0.21$ (50% EtOAc/hexanes). **IR** (FT-ATR, cm^{-1}): 3310, 3090, 2819, 1661, 1591, 1570, 1291, 1112, 933. **¹H-NMR** (400 MHz, $\text{DMSO}-d_6$): δ 9.85 (s, 1H), 8.10 (dd, $J = 7.9, 1.5\text{ Hz}$, 1H), 7.84 (ddd, $J = 8.4, 7.1, 1.6\text{ Hz}$, 1H), 7.66 (dd, $J = 8.3, 1.1\text{ Hz}$, 1H), 7.52 (ddd, $J = 8.3, 7.2, 1.2\text{ Hz}$, 1H), 7.36 (t, $J = 8.0\text{ Hz}$, 1H), 6.92 (ddd, $J = 8.3, 2.4, 1.0\text{ Hz}$, 1H), 6.84 (ddd, $J = 7.8, 2.0, 0.9\text{ Hz}$, 1H), 6.80 (t, $J = 2.1\text{ Hz}$, 1H), 2.17 (s, 3H). **¹³C-NMR** (151 MHz, $\text{DMSO}-d_6$): δ 161.6, 158.7, 154.9, 147.7, 139.2, 134.9, 130.7, 127.1, 126.8, 126.7, 120.9, 119.2, 116.4, 115.8, 24.2. **HRMS:** Exact mass calculated for $[\text{C}_{15}\text{H}_{12}\text{N}_2\text{O}_2 + \text{H}]^+$ requires $m/z = 253.0977$. Found 253.0975 (ESI+).

IV. Bromination Procedures and Characterization of Tribromide 2

A. Peptide Screening Procedure



To an oven-dried 20 mL vial equipped with a magnetic stir bar was added 3-(3-hydroxyphenyl)-2-methyl-quinazolin-4(3H)-one (**1**, 12.6 mg, 0.050 mmol) and peptide catalyst (0.005 mmol, 10 mol% w.r.t. **1**). The solid mixture was suspended in 5 mL of PhMe/CHCl₃ (9:1 v/v, 0.01 M w.r.t. **1**), and the resulting suspension was allowed to stir vigorously at rt. *N*-Bromosuccinimide (NBS, 26.7 mg, 0.15 mmol, 3.0 equiv w.r.t. **1**) was added in one portion to the stirring solution at rt. The vial was sealed with a cap, and the reaction solution was allowed to stir for 60 minutes. (Note: A color change from colorless to yellow was observed within 15 minutes. In some cases, the clear yellow or pale yellow reaction solutions turned cloudy.) The reaction was quenched by addition of 1 mL of MeOH followed by (trimethylsilyl)diazomethane solution (TMSCHN₂, 2.0 M in hexanes) until the bright yellow color persisted in solution (Note: the yellow reaction solution became clear and colorless before turning bright yellow). The solution was allowed to stir 15–20 minutes at rt, after which glacial acetic acid was added dropwise until the solution became clear and colorless. The solvent was removed *in vacuo*, and the crude reaction mixture was purified by flash chromatography through a pipette silica plug (1 x 6 cm SiO₂) washing with EtOAc/hexanes (1:1 v/v). The fractions were pooled and concentrated *in vacuo*. The resulting white foam (or clear oil) was dried thoroughly on high vacuum to provide 3-(2,4,6-tribromo-3-methoxyphenyl)-2-methyl-quinazolin-4(3H)-one (**2**), which was analyzed by chiral HPLC to assess the enantioselectivity of the reaction. **Chiral HPLC** (Chiralcel OJ-H column, 10% EtOH/hexanes eluent, 2 mL injection, 1 mLmin⁻¹ flow rate, regulated at 20 °C, 230 nm): major enantiomer *t*_R = 9.7 min, minor enantiomer *t*_R = 12.6 min. (Note: Conversion of **1** was always complete, and thus only *er* values were tabulated in Figure 2 and Figure S1.).

B. Cumulative Peptide Screening Data

Figure S1 presents our cumulative peptide results from this work, as well as our previous report.⁶ All results were obtained using the Peptide Screening Procedure described above (section IV.A).

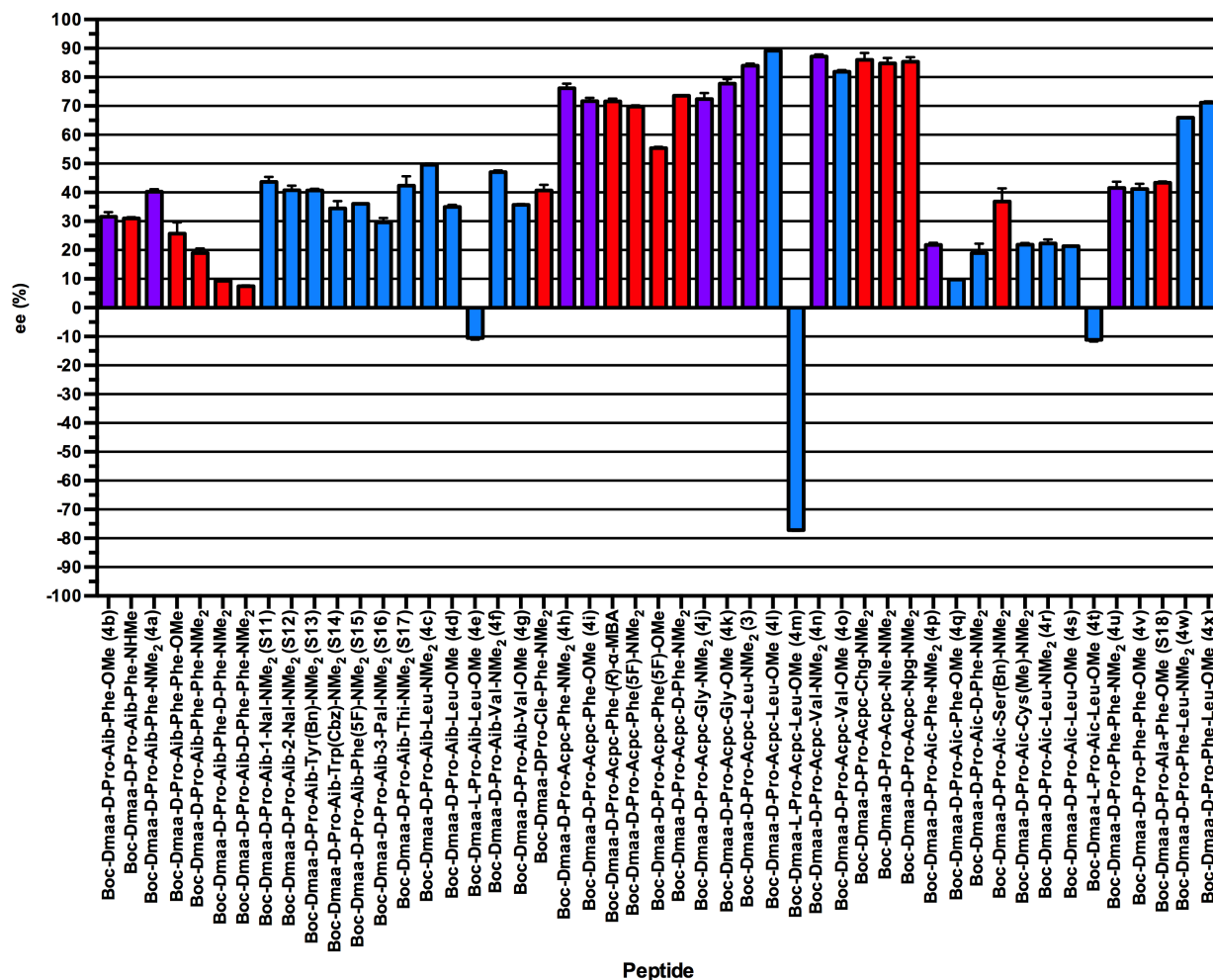
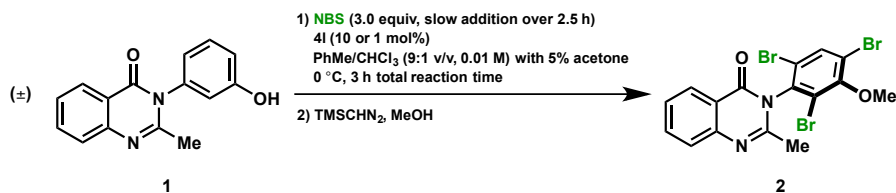


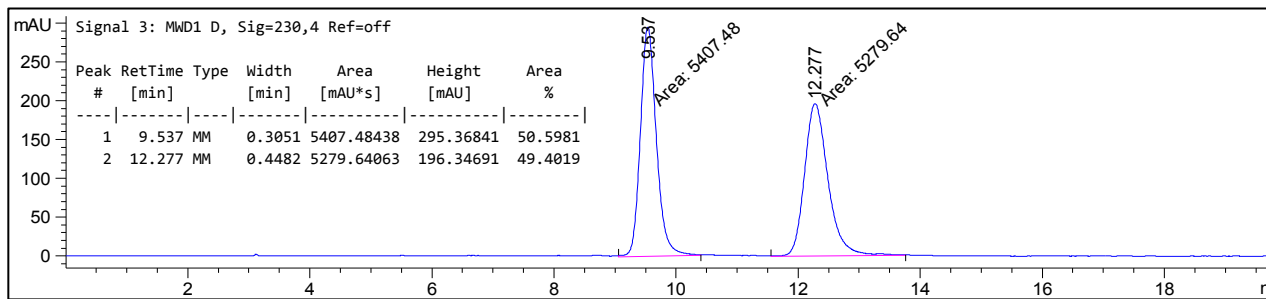
Figure S1: Cumulative peptide screening data for the atroposelective bromination of **1**. New entries from this study are presented in **blue**. Entries from ref. 6 are presented in **red**. Entries that appear in both ref. 6 and this study are in **purple**.

C. Preparative Bromination Procedure Using 4I

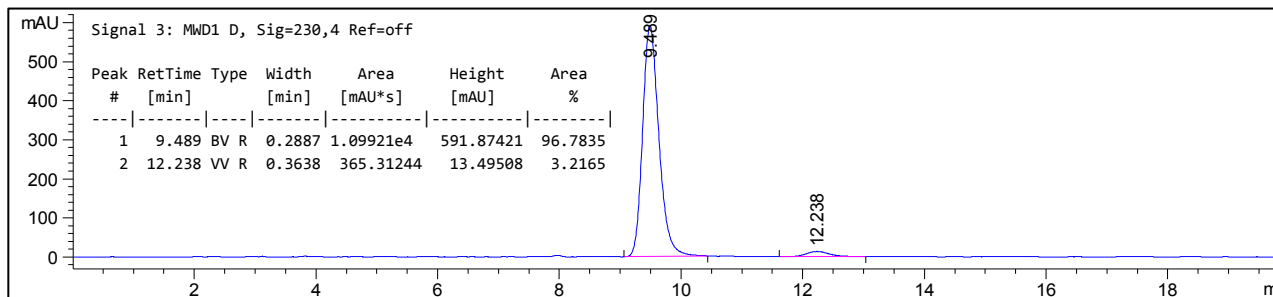


N-Bromosuccinimide (NBS, 53.3 mg, 0.30 mmol, 3.0 equiv w.r.t. **1**) was added to a 10 mL scintillation vial shielded from light, and 3.5 mL of PhMe/CHCl₃ (9:1 v/v) were added to the vial. The suspension of NBS was allowed to stir as 0.5 mL of acetone was added (to facilitate dissolution of NBS). The vial was sealed with a PTFE-lined cap, and the contents were allowed to stir at rt. Complete NBS dissolution typically required 5–10 minutes. In the meantime, quinazolinone **1** (25.2 mg, 0.10 mmol) and Boc-Dmaa-D-Pro-Acpc-Leu-OMe (**4I**, 5.4 mg, 0.01 mmol, 10 mol% w.r.t. **1** or 0.54 mg, 0.001 mmol, 1 mol% w.r.t. **1**) were added to a flame-dried 50 mL round bottom flask equipped with a magnetic stir bar. The solid mixture was suspended in 6 mL of PhMe/CHCl₃ (9:1 v/v), and the resulting cloudy suspension was allowed to stir vigorously under N₂ at 0 °C. Once the NBS was *completely dissolved*, the delivery solution was taken up into a 5 mL syringe (12.46 mm diameter) and delivered into the substrate/peptide solution over 150 minutes (1.6 mLh⁻¹) at 0 °C using a syringe pump (Note: An 18 G needle was used to avoid clogging by NBS precipitation). During this time, the syringe was shielded from light using aluminum foil and the lights within the fume hood were turned off. After the addition was complete, the clear, colorless yellow solution was allowed to stir 30 minutes at under N₂. The reaction was quenched by addition of 2 mL of MeOH, followed by (trimethylsilyl)diazomethane solution (TMSCHN₂, 2 M in hexanes) until the bright yellow color persisted in solution. The solution was allowed to stir 15–20 minutes at rt, after which glacial acetic acid was added dropwise until the solution became clear and colorless. The solvent was removed *in vacuo*, and the crude reaction mixture was purified by flash chromatography on a Biotage Isolera One instrument (10 g SNAP Ultra column, 7–60% EtOAc/hexanes over 12 column volumes, loading in dichloromethane). The appropriate fractions were pooled, concentrated *in vacuo*, and dried thrice azeotropically with dichloromethane. The resulting white foam was dried thoroughly on high vacuum to provide 2-Methyl-3-(2,4,6-tribromo-3-methoxyphenyl)-quinazolin-4(3H)-one (**2**)⁶ as a foamy, white solid in 92% yield when 10 mol% of **4I** was used and 80% yield when 1 mol% of **4I** was used. **TLC**: R_f = 0.32 (30% EtOAc/hexanes). **IR** (FT-ATR, cm⁻¹): 3067, 2937, 1690, 1605, 1569, 1371, 996. **¹H-NMR** (400 MHz, CDCl₃): δ 8.29 (dd, *J* = 8.0, 1.4 Hz, 1H), 7.98 (s, 1H), 7.80 (ddd, *J* = 8.5, 7.1, 1.5 Hz, 1H), 7.71 (d, *J* = 8.1 Hz, 1H), 7.56 – 7.43 (m, 1H), 3.95 (s, 3H), 2.22 (s, 3H). **¹³C-NMR** (101 MHz, CDCl₃): δ 160.3, 155.4, 152.5, 147.5, 136.9, 135.9, 135.1, 127.3, 127.1, 126.9, 120.8, 120.4, 120.1, 118.8, 61.0, 22.9. **HRMS**: Exact mass calculated for [C₁₆H₁₁N₂O₂Br₃ + H]⁺ requires *m/z* = 500.8448. Found 500.8449 (ESI+). **Optical**: [α]_D²⁰ = +24.3 (*c* = 0.75, CH₂Cl₂, 97:3 er). **HPLC** (Chiralcel OJ-H column, 10% EtOH/hexanes eluent, 2 μL injection, 1 mLmin⁻¹ flow rate, regulated at 20 °C, 230 nm): major enantiomer t_R = 9.5 min, minor enantiomer t_R = 12.4 min, 97:3 er (10 mol% **4I**) and 97:3 er (1 mol% **4I**).

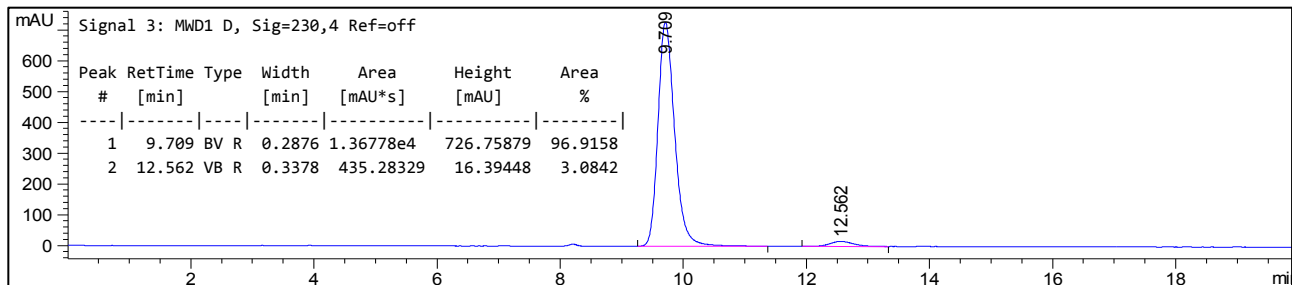
Racemic:



Enantioenriched using 10 mol% of 4I:



Enantioenriched using 1 mol% of 4I:



V. Solution-Phase NMR Studies of **3** and **4I**

A. NMR Methods

To fully characterize peptides in solution, one-dimensional ^1H and two-dimensional gCOSY and NOESY experiments were carried out for each compound. All data were collected on Varian Inova 600 MHz spectrometers that were equipped with VnmrJ, version 4.2 revision A. Varian provided the pulse sequences for all experiments. All samples were prepared in C_6D_6 (with C_6H_6 set to 7.15 ppm)¹ at a concentration of 0.01 M, which was demonstrated to be below the aggregation limit for these peptides.

The NOESY spectra for **3** and **4I** were acquired at 25 °C and 20 °C, respectively, the difference in temperatures being the result of instrument defaults at the time of acquisition. NOESY data for each peptide was collected with a mixing time of 300 ms, a spectral width of 9615.4 Hz, and a d1 time of 3 s. The data was acquired with a total of 256 transients, 1442 points in the f2 dimension, and 256 points in the f1 dimension. The spectra were processed using MestReNova, version 9.0.0-12821. Zero-filling sized the spectra to 2048, 2048. Automatic phasing was used in conjunction with manual adjustments. Additionally, apodization was accomplished with a sine square function (90°) in both dimensions. Each spectrum was automatically baseline corrected in each dimension using the Bernstein third order polynomial fit and treated with COSY-like symmetrization. The NOESY spectra of **3** and **4I** were inspected before and after symmetrization, and peaks deemed to be artifacts were discarded. Two peaks, both of which appeared in t1 ridges in the unsymmetrized data, were discarded from the analysis of peptide **4I**. Further refinement included treatment of the spectrum to reduce t1 noise.

NOESY spectra were integrated to extract distances from observed through-space interactions between protons on each peptide. After integrating NOESY cross-peaks, the peaks' volumes were converted to distances using the equation (ESI-1),⁷ where r_{ij} is the calculated distance, r_{ref} is a reference distance, v_{ref} is the volume of a reference peak, and v_{ij} is the volume of the cross-peak in question. Reference peaks were chosen to be those that corresponded to interactions between δ -protons on the peptide's respective D-Pro residue. Reference distances that corresponded to these volumes were extracted from the appropriate peptide crystal structure.

$$r_{ij} = r_{ref} \sqrt[6]{\left(\frac{v_{ref}}{v_{ij}}\right)} \quad (\text{ESI-1})$$

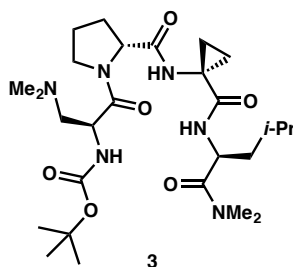
Integrated volumes were corrected using equation (ESI-2),⁸ where v is the volume corresponding to either the reference or the peak in question from ESI-1, v_{raw} is the uncorrected volume of a peak in question, and v_{diag1} and v_{diag2} correspond to the volumes of the diagonal peaks for each respective interacting proton.

$$\nu = \frac{2\nu_{raw}}{(\nu_{diag1} + \nu_{diag2})} \quad (\text{ESI-2})$$

The restraints were then processed using the standard *Crystallography and NMR Systems* (CNS)⁹ simulated annealing protocol. A parameter file for each residue was assembled within the program. Each peptide was treated with the macro commands generate_seq, generate_extended, and anneal. By altering the energy-scoring threshold in the program's accept input file, we were able to cull the 10-lowest energy scored conformations for each structure. The accept feature of CNS also generated the average structure of these 10 conformers, which in turn, became the input for DFT calculations. Bins were defined at 1.8 to 2.5 Å, 1.8 to 3.0 Å, 1.8 to 3.5 Å, and 1.8 to 4.5 Å. Distances that were calculated to be over 4.5 Å were not included in the CNS restraint file.

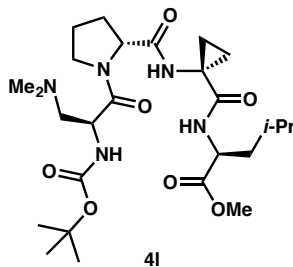
The simulated annealing outputs from CNS were then used as a starting geometries for optimization and frequency calculation at the B3LYP/6-31G(d,p) level of theory using Gaussian 09.^{10,11} Benzene was specified as the implicit solvent using the IEFPCM protocol.¹² Each structure was restrained using nOe-derived redundant internal coordinates. For peptide **3**, the following redundant internal coordinates were specified: NH_{Leu} to NH_{Dmaa} was restrained to 3.3 Å, β_{Dmaa} to β_{Leu} was restrained to 3.9 Å, and NH_{Leu} to α_{D-Pro} was restrained to 3.9 Å. For peptide **4I**, the following redundant internal coordinates were specified: NH_{Leu} to NH_{Dmaa} was restrained to 4.2 Å, NH_{Leu} to NH_{Acpc} was restrained to 3.2 Å, and NH_{Leu} to α_{D-Pro} was restrained to 3.7 Å. The optimization outputs were subsequently checked for consistency with the nOe-derived distances. In most cases, the optimized structures were in good accord with the NMR restraints.

B. Full ¹H-NMR Assignment of Peptides 3 and 4I



¹H-NMR (600 MHz, 0.01 M in C₆D₆, 25 °C):⁶ δ 8.06 (d, J = 8.7 Hz, 1H, NH_{Leu}), 7.10 (d, J = 7.2 Hz, 1H, NH_{Dmaa}), 6.74 (s, 1H, NH_{Acpc}), 5.25 (td, J = 9.2, 4.8 Hz, 1H, α_{Leu}), 4.56 (q, J = 7.4 Hz, 1H, α_{Dmaa}), 4.13 (dd, J = 8.7, 4.9 Hz, 1H, α_{D-Pro}), 3.76 (dt, J = 9.8, 6.2 Hz, 1H, δ_{D-Pro}), 3.22 (dt, J = 9.6, 7.1 Hz, 1H, δ'_{D-Pro}), 2.87 (dd, J = 12.0, 6.0 Hz, 1H, β_{Dmaa}), 2.66 (s, 3H, NMe_{Leu}), 2.63 (s, 3H, NMe'_{Leu}), 2.54 (dd, J = 12.3, 6.4 Hz, 1H, β'_{Dmaa}), 2.12 (dd, J = 13.6, 4.8 Hz, 1H, β_{Leu}), 2.09 (s, 6H, 2x NMe_{Dmaa}), 2.04 (dtd, J = 8.4, 6.5, 4.9 Hz, 1H, γ_{Leu}), 1.93 – 1.87 (m, 1H, β_{Aic}), 1.78 (dt, J = 10.8, 3.8 Hz, 1H, β'_{Dmaa}), 1.72 (dt, J = 12.3, 6.1 Hz, 1H, β_{D-Pro}), 1.63 (ddd, J = 15.3, 7.6, 3.3 Hz, 1H, β'_{Leu}), 1.57 (dt, J = 14.4, 7.3 Hz, 1H, γ_{D-Pro}), 1.51 (s, 9H, $t-Bu_{Dmaa}$), 1.49 – 1.42 (m, 1H, β'_{D-}

Pro), 1.19 (dt, $J = 12.4, 6.3$ Hz, 1H, γ' _{D-Pro}), 1.02 (dd, $J = 9.2, 6.6$ Hz, 6H, δ _{Leu}), 0.96 – 0.89 (m, 2H, β'' _{Acpc}).



¹H-NMR (600 MHz, 0.01 M in C₆D₆, 20 °C): δ 7.93 (d, $J = 7.8$ Hz, 1H, NH_{Leu}), 7.67 (s, 1H, NH_{Acpc}), 5.82 (s, 1H, NH_{Dmaa}), 5.06 (ddd, $J = 10.0, 7.8, 4.6$ Hz, 1H, α_{Leu}), 4.42 (dd, $J = 8.7, 4.4$ Hz, 1H, α_{D-Pro}), 4.13 – 4.07 (m, 1H, α_{Dmaa}), 3.62 (td, $J = 8.6, 5.0$ Hz, 1H, δ_{D-Pro}), 3.36 (s, 3H, OMe_{Leu}), 2.91 (q, $J = 8.3$ Hz, 1H, δ'_{D-Pro}), 2.45 (dd, $J = 12.2, 9.0$ Hz, 1H, β_{Dmaa}), 2.28 – 2.22 (m, 1H, β_{Acpc}), 2.18 (m, 1H, γ_{Leu}), 2.16 (m, 1H, β_{Leu}), 2.11 (dd, $J = 11.8, 5.8$ Hz, 1H, β'_{Dmaa}), 1.82 (s, 6H, 2 x NMe_{Dmaa}), 1.80 (m, 1H, β'_{Leu}), 1.79 (m, 1H, β_{D-Pro}), 1.68 – 1.65 (m, 1H, β'_{Acpc}), 1.65 – 1.59 (m, 1H, β'_{D-Pro}), 1.53 (s, 9H, $t-Bu_{Dmaa}$), 1.46 – 1.38 (m, 1H, γ_{D-Pro}), 1.22 – 1.17 (m, 1H, β''_{Acpc}), 1.16 – 1.11 (m, 1H, γ'_{D-Pro}), 1.06 (ddd, $J = 10.1, 7.6, 4.1$ Hz, 1H, β'''_{Acpc}), 1.00 (dd, $J = 30.0, 6.3$ Hz, 6H, δ_{Leu}).

C. Tabular Representation of NOESY Cross-Peaks and Their Corresponding ^1H to ^1H Distances

The notation used below is as follows: each proton is designated by the three-letter code of its amino acid residue. Protons on the *tert*-butoxycarbonyl (Boc) *N*-terminal cap are called BocMe protons. Additional notation equates the following: A= α , B= β , C= γ , D= δ . Finally, for protons that are on the same carbon but are NMR-distinct, “1” is attributed to the more downfield proton and “2” to the more upfield proton. As an example, LeuHB1 is the notation for the more downfield β -proton of the leucine residue in our peptide. The NOESY spectrum and nOe-map for each peptide is shown below. Each nOe map is accompanied by a legend that color-codes the distance between the protons whose through-space interactions were detected by our NOESY experiments.

Peptide 3

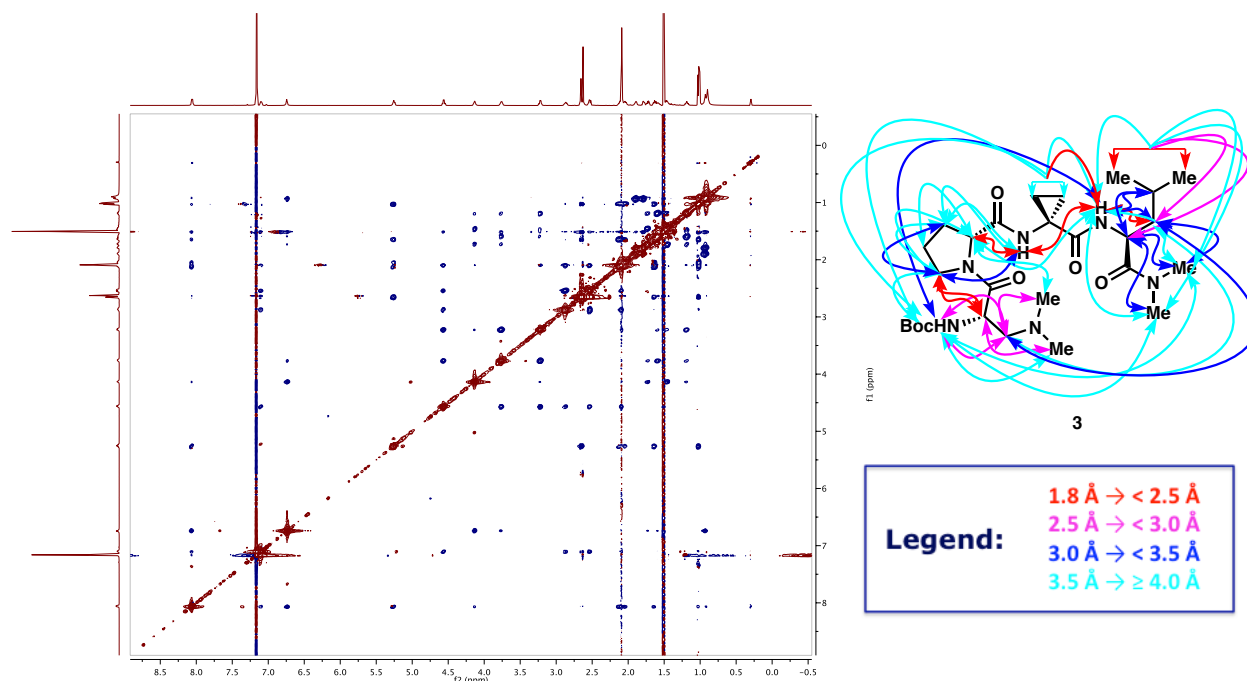


Table S1: NOESY-Derived Distances and Assignments for Peptide

	f2	f1	Normalized	Absolute	Assignment	Corrected Distances (Normalized)
1	8.06	1.04	-0.54	-0.29	LeuNH-LeuHD	4.29
	1.02	8.06	-0.64	-0.34		
2	8.06	0.92	-0.48	-0.26	LeuNH-AcpcHB1	3.66
	0.91	8.07	-0.52	-0.28		
3	8.06	7.11	-1	-0.53	LeuNH-DmaaNH	3.26
	7.11	8.08	-0.97	-0.52		
4	8.06	6.75	-5.67	-3.02	LeuNH-AcpcNH	2.42
	6.73	8.08	-5.58	-2.97		
5	8.06	2.04	-1.78	-0.95	LeuNH-LeuHC	3.00
	2.03	8.06	-1.7	-0.91		
6	8.06	2.11	-4.37	-2.32	LeuNH-LeuHB1	2.39
	2.11	8.06	-4.59	-2.44		
7	8.05	4.14	-0.4	-0.21	LeuNH-DProHA	3.89
	4.12	8.06	-0.36	-0.19		

8	8.05	1.65	-1.09	-0.58	LeuNH-LeuHB2	3.20
	1.64	8.07	-1.04	-0.56		
9	8.05	2.66	-0.1	-0.05	LeuNH-LeuNMe2	4.96
	2.65	8.06	-0.11	-0.06		
10	8.05	2.63	-0.08	-0.04	LeuNH-LeuNMe1	5.27
	2.63	8.06	-0.09	-0.05		
11	7.1	2.09	-0.81	-0.43	DmaaNH-DmaaMe	4.02
	2.09	7.1	-0.74	-0.39		
12	7.1	2.89	-2.51	-1.33	DmaaNH-DmaaHB2	2.78
	2.87	7.11	-2.57	-1.37		
13	7.1	2.66	-0.21	-0.11	DmaaNH-LeuNMe2	4.53
	2.66	7.1	-0.17	-0.09		
14	7.1	2.54	-2.56	-1.36	DmaaNH-DmaaHB1	2.80
	2.53	7.1	-2.69	-1.43		
15	7.1	2.63	-0.57	-0.3	DmaaNH-LeuNMe1	3.87
	2.63	7.1	-0.56	-0.3		
16	6.73	0.93	-5.4	-2.87	AcpcNH-AcpcHB1	2.48
	0.93	6.75	-5.35	-2.85		
17	6.73	3.77	-0.93	-0.49	AcpcNH-DProHD2	3.29
	3.76	6.74	-0.94	-0.5		
18	6.73	1.61	-0.44	-0.23	AcpcNH-DProHB1	3.68
	1.58	6.74	-0.49	-0.26		
19	6.73	1.73	-0.52	-0.27	AcpcNH-DProHB2	3.73
	1.72	6.74	-0.44	-0.23		
20	6.73	4.14	-7.81	-4.16	AcpcNH-DProHA	2.36
	4.11	6.75	-7.78	-4.14		
21	5.25	2.63	-2.6	-1.38	LeuHA-LeuNMe1	3.00
	2.63	5.26	-3.14	-1.67		
22	5.25	1.02	-8.02	-4.27	LeuHA-LeuHD	2.81
	1.02	5.26	-7.98	-4.24		
23	5.25	2.67	-8.26	-4.39	LeuHA-LeuNMe2	3.43
	2.67	5.26	-8.25	-4.39		
24	5.25	2.04	-2.02	-1.07	LeuHA-LeuHC	3.02
	2.04	5.26	-2.04	-1.09		
25	4.57	3.22	-9.7	-5.16	DmaaHA-DProHD1	2.26
	3.22	4.57	-9.66	-5.14		
26	4.56	3.76	-8.64	-4.6	DmaaHA-DProHD2	2.31
	3.76	4.57	-8.65	-4.6		
27	4.56	2.1	-7.21	-3.83	DmaaHA-DmaaMe	2.78
	2.09	4.58	-7.17	-3.81		
28	4.13	3.23	-0.52	-0.28	DProHA-DProHD1	3.70
	3.22	4.13	-0.54	-0.29		
29	4.13	1.2	-0.79	-0.42	DProHA-DProHC1	3.50
	1.19	4.14	-0.85	-0.45		
30	4.13	2.1	-0.25	-0.13	DProHA-DmaaMe	4.97
	2.09	4.14	-0.2	-0.1		
31	3.76	1.73	-1.12	-0.6	DProHD2-DProHB2	3.50
	1.72	3.76	-1.13	-0.6		
32	3.76	1.51	-0.73	-0.39	DProHD2-BocMe	4.30
	1.51	3.76	-0.73	-0.39		
33	3.22	1.46	-1.25	-0.66	DProHD1-DProHB1	3.18
	1.46	3.22	-1.25	-0.66		
34	2.88	1.64	-0.29	-0.15	DmaaHB2-LeuHB2	3.93
	1.64	2.87	-0.33	-0.17		
35	2.87	2.1	-8.64	-4.59	DmaaHB2-DmaaMe	2.68
	2.09	2.87	-8.47	-4.51		
36	2.66	1.63	-1.57	-0.84	LeuNMe2-LeuHB2	3.20
	1.64	2.66	-1.47	-0.78		
37	2.65	1.02	-1.31	-0.69	LeuNMe2-LeuHD	4.10
	1.01	2.66	-1.26	-0.67		
38	2.62	1.02	-0.43	-0.23	LeuNMe1-LeuHD	4.59
	1.02	2.63	-0.52	-0.28		
39	2.54	2.1	-7.49	-3.98	DmaaHB1-LeuHB2	2.93
	2.09	2.53	-7.55	-4.02		
40	1.64	1.02	-7.41	-3.94	LeuHB2-LeuHD	2.82
	1.02	1.64	-7.67	-4.08		
41	1.51	1.79	-1.53	-0.75	BocMe-AcpcHB	3.79

	1.79	1.51	-1.55	-0.76		
42	1.51	0.92	-1.13	-0.56	BocMe-AcpcHB	4.00
	0.93	1.5	-1.15	-0.56		
43	3.77	3.23	-35.57	-18.91	DProHD1-DProHD2	1.80
	3.22	3.79	-35.4	-18.82		

Peptide 4I

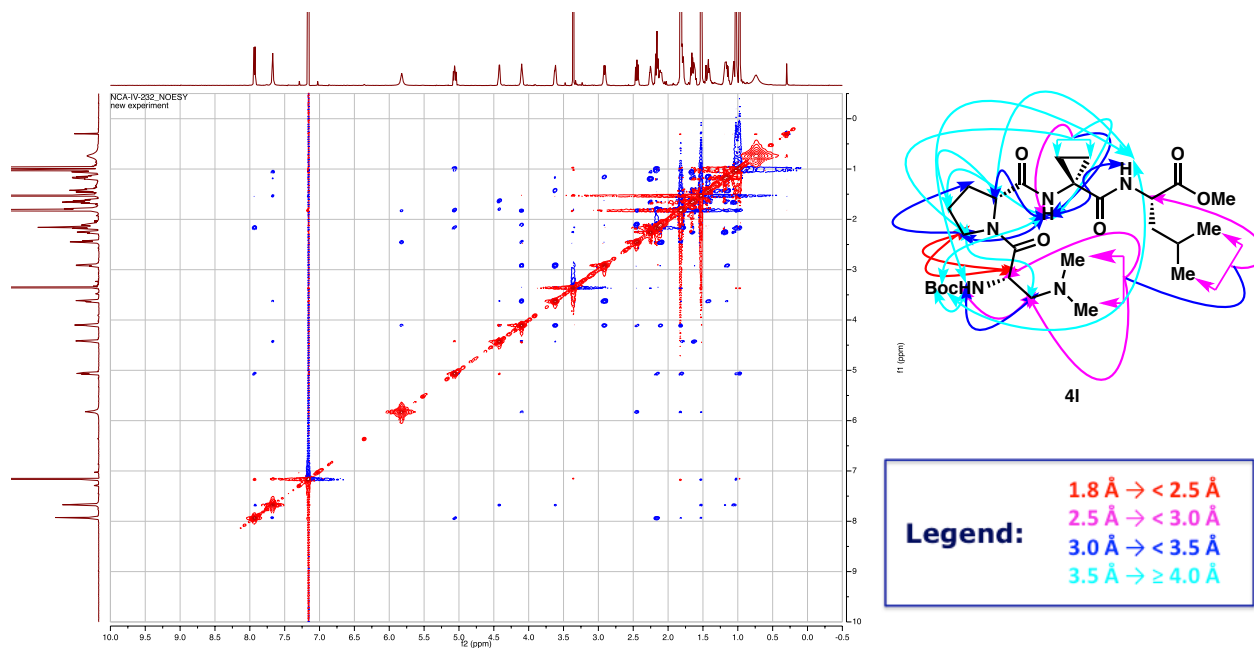


Table S2: NOESY-Derived Distances and Assignments for Peptide 4I

	f2	f1	Normalized	Absolute	Assignment	Corrected Distances (Normalized)
1	7.93	5.81	-0.24	-0.03	LeuNH-DmaaNH	4.21
	5.81	7.94	-0.24	-0.03		
2	7.93	7.67	-1.27	-0.18	LeuNH-AcpcNH	3.19
	7.67	7.93	-1.26	-0.18		
3	7.93	1.53	-0.72	-0.1	LeuNH-BocMe	4.31
	1.53	7.93	-0.7	-0.1		
4	7.93	4.42	-0.55	-0.08	LeuNH-DProHA	3.70
	4.42	7.93	-0.58	-0.08		
5	7.67	1.53	-1.75	-0.25	AcpcNH-BocMe	3.70
	1.53	7.67	-1.75	-0.25		
6	7.67	1.42	-0.95	-0.14	AcpcNH-DProHC2	3.60
	1.42	7.67	-0.9	-0.13		
7	7.67	1.06	-4.47	-0.64	AcpcNH-AcpcHB1a	2.55
	1.05	7.67	-4.48	-0.64		
8	7.67	4.42	-1.76	-0.25	AcpcNH-DProHA	3.03
	4.42	7.67	-1.76	-0.25		
9	7.67	3.62	-1.63	-0.23	AcpcNH-DProHD2	3.04
	3.62	7.67	-1.63	-0.23		
10	7.67	1.18	-1.09	-0.16	AcpcNH-AcpcHB1b	3.32
	1.18	7.67	-1.11	-0.16		
11	7.67	1.66	-0.28	-0.04	AcpcNH-AcpcHB2a	4.18
	1.66	7.67	-0.28	-0.04		
12	5.82	2.45	-5.57	-0.8	DmaaNH-DmaaHB2	2.51

	2.45	5.83	-5.55	-0.8		
13	5.82	1.53	-0.91	-0.13	DmaaNH-BocMe	4.13
	1.53	5.82	-0.9	-0.13		
14	5.81	2.1	-1.35	-0.19	DmaaNH-DmaaHB1	3.15
	2.1	5.82	-1.31	-0.19		
16	5.06	0.99	-6.49	-0.93	LeuHA-LeuHD	2.73
	0.99	5.06	-6.57	-0.94		
17	4.1	3.62	-13.32	-1.92	DmaaHA-DProHD2	2.18
	3.62	4.1	-13.33	-1.92		
18	4.42	1.42	-0.19	-0.03	DProHA-DProHC2	4.62
	1.41	4.42	-0.18	-0.03		
19	4.1	2.91	-10.44	-1.5	DmaaHA-DProHD1	2.28
	2.91	4.1	-10.38	-1.49		
20	4.1	1.82	-7.1	-1.02	DmaaHA-DmaaMe	2.87
	1.82	4.11	-7.11	-1.02		
21	3.61	1.06	-0.27	-0.04	DProHD2-AcpcHB1a	4.10
	1.06	3.62	-0.27	-0.04		
23	2.91	1.62	-0.9	-0.13	DProHD1-DProHB1	3.31
	1.61	2.91	-0.96	-0.14		
24	2.91	2.11	-0.65	-0.09	DProHD1-DmaaHB1	3.60
	2.11	2.91	-0.64	-0.09		
25	2.44	1.82	-5.64	-0.81	DmaaHB2-DmaaMe	2.99
	1.82	2.44	-5.64	-0.81		
26	1.81	1.02	-6.61	-0.95	LeuHD(downfield)-DmaaMe	3.04
	1.02	1.82	-6.59	-0.95		
27	3.62	2.91	-40.93	-5.89	DProHD2-DProHD1	1.80
	2.91	3.61	-40.67	-5.85		

D. Ten Lowest-Energy Scored Structures from Simulated Annealing with CNS

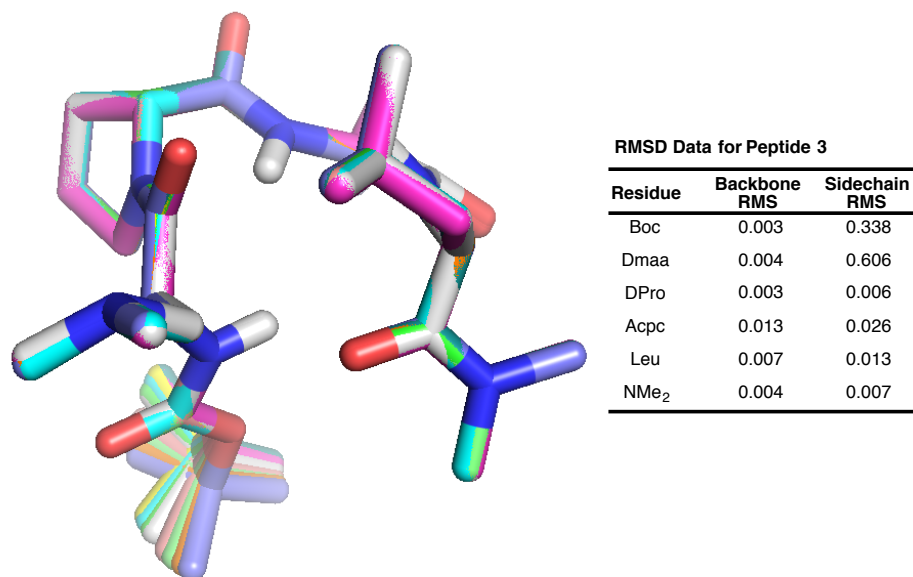


Figure S2: Ten lowest-energy scored structures from simulated annealing of peptide **3** in CNS. The ensemble shows a high degree of homogeneity across all ten structures with the most variability being in the Boc *N*-terminal cap.

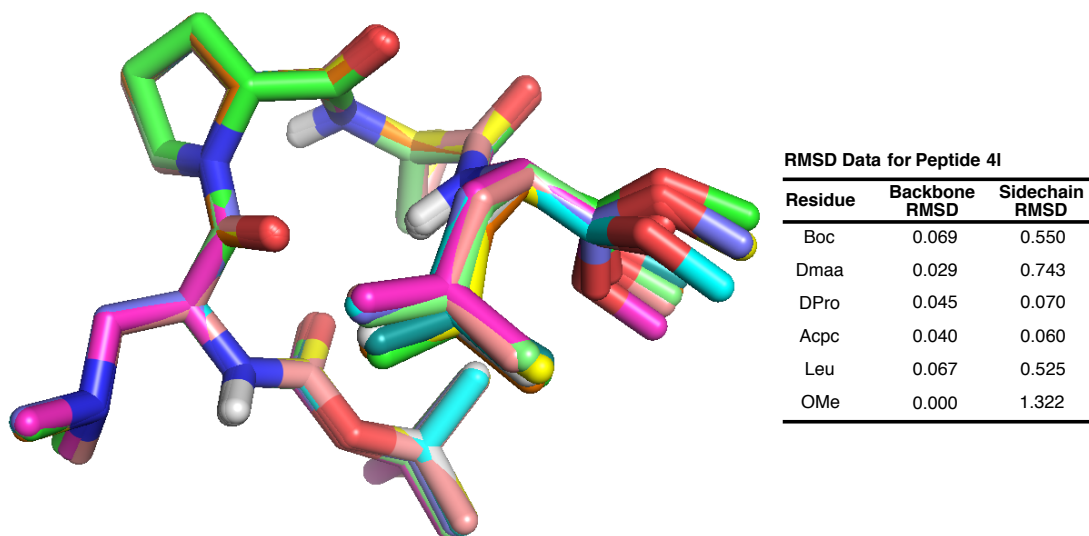


Figure S3: Ten lowest energy-scored structures from simulated annealing of peptide **4I** in CNS. The ensemble shows a high degree of homogeneity across all ten structures with the most variability being in the methyl-ester *C*-terminal cap.

E. CNS Simulated Annealing Outputs

Table S3: CNS-Output Coordinates for Peptide 3*

Tag	Symbol	X	Y	Z	Tag	Symbol	X	Y	Z
1	O	5.985	-1.441	-1.017	61	H	11.666	0.745	1.294
2	C	7.155	-1.126	-1.23	62	C	12.356	-1.022	0.374
3	O	7.721	-0.944	-2.445	63	H	13.297	-1.133	-0.103
4	C	6.891	-0.866	-3.654	64	C	12.421	-1.679	1.739
5	C	6.13	-2.179	-3.838	65	H	13.444	-1.658	2.073
6	C	5.894	0.285	-3.52	66	H	12.109	-2.713	1.617
7	C	7.812	-0.625	-4.842	67	C	11.554	-1.046	2.819
8	H	6.683	-2.822	-4.505	68	H	10.695	-0.583	2.358
9	H	5.158	-1.973	-4.258	69	C	11.058	-2.111	3.781
10	H	6.011	-2.671	-2.882	70	H	10.108	-1.809	4.194
11	H	5.058	0.111	-4.179	71	H	11.775	-2.239	4.577
12	H	6.38	1.21	-3.789	72	H	10.939	-3.044	3.247
13	H	5.541	0.347	-2.5	73	C	12.341	0.028	3.546
14	H	7.306	-0.004	-5.565	74	H	11.682	0.839	3.815
15	H	8.068	-1.571	-5.293	75	H	13.121	0.397	2.893
16	H	8.715	-0.129	-4.511	76	H	12.785	-0.391	4.437
17	N	8.048	-0.929	-0.265	77	C	11.457	-1.806	-0.46
18	H	8.943	-0.611	-0.51	78	O	10.298	-2.057	-0.131
19	C	7.643	-0.847	1.132	79	N	12.056	-2.368	-1.486
20	H	6.565	-0.858	1.169	80	C	11.354	-3.226	-2.302
21	C	8.185	-2.055	1.901	81	C	13.453	-2.114	-1.873
22	H	9.226	-1.877	2.138	82	H	12.062	-3.759	-2.888
23	H	8.122	-2.923	1.264	83	H	10.842	-3.884	-1.635
24	N	7.491	-2.352	3.119	84	H	10.659	-2.683	-2.925
25	C	6.046	-2.508	2.955	85	H	13.611	-1.052	-1.973
26	H	5.846	-3.168	2.126	86	H	14.112	-2.509	-1.115
27	H	5.6	-1.542	2.765	87	H	13.667	-2.596	-2.818
28	H	5.623	-2.93	3.854					
29	C	8.036	-3.502	3.84					
30	H	7.52	-4.399	3.535					
31	H	7.905	-3.353	4.903					
32	H	9.086	-3.605	3.617					
33	C	8.148	0.45	1.761					
34	O	8.813	0.436	2.796					
35	N	7.842	1.603	1.136					
36	C	8.253	2.911	1.602					
37	H	8.467	2.906	2.645					
38	C	7.032	3.739	1.301					
39	H	7.332	4.739	1.041					
40	H	6.42	3.751	2.17					
41	C	6.345	3.055	0.149					
42	H	6.41	3.677	-0.73					
43	H	5.311	2.87	0.399					
44	C	7.065	1.747	-0.084					
45	H	7.709	1.822	-0.945					
46	H	6.367	0.938	-0.196					
47	C	9.45	3.425	0.844					
48	O	9.925	4.534	1.091					
49	N	10.16	2.438	0.403					
50	H	9.81	1.561	0.63					
51	C	11.262	2.419	-0.587					
52	C	11.92	3.734	-0.981					
53	C	11.017	3.02	-1.964					
54	H	11.498	4.688	-0.701					
55	H	12.917	3.789	-1.388					
56	H	11.574	2.7	-2.832					
57	H	10.164	3.641	-2.183					
58	C	12.183	1.223	-0.571					
59	O	12.84	0.939	-1.572					
60	N	11.993	0.388	0.447					

*Average of the 10 lowest-energy scored structures generated by CNS.

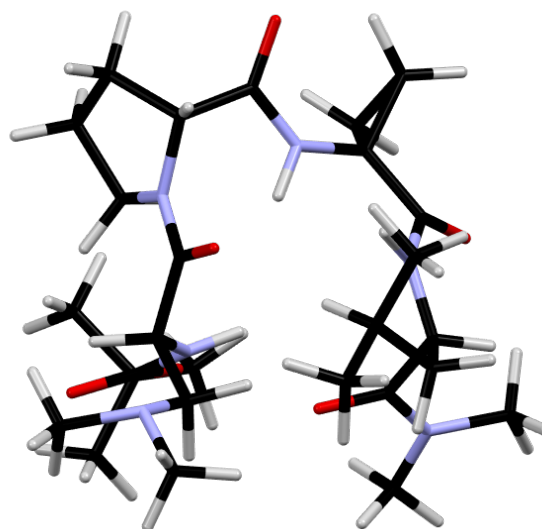
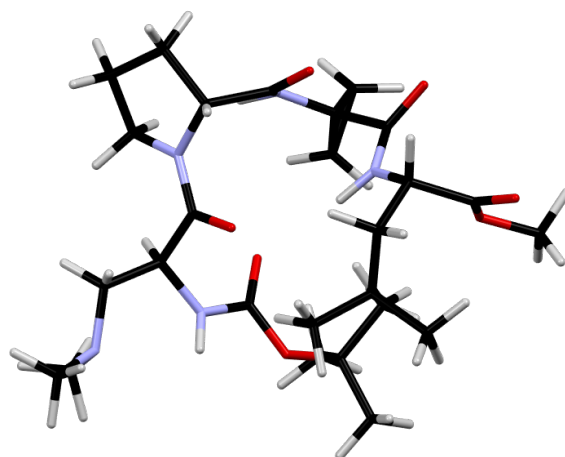


Table S4: CNS-Output Coordinates for Peptide 4I*

Tag	Symbol	X	Y	Z	Tag	Symbol	X	Y	Z
1	O	6.988	0.569	-1.485	64	C	10.807	-2.512	0.478
2	C	6.605	-0.598	-1.568	65	H	10.162	-2.345	1.327
3	O	6.868	-1.451	-2.584	66	H	11.51	-3.294	0.728
4	C	7.613	-0.999	-3.766	67	C	9.945	-2.995	-0.69
5	C	6.854	0.14	-4.446	68	H	9.649	-2.144	-1.287
6	C	8.996	-0.506	-3.343	69	C	10.735	-3.941	-1.581
7	C	7.746	-2.179	-4.718	70	H	10.505	-4.962	-1.316
8	H	7.252	0.293	-5.437	71	H	11.792	-3.764	-1.447
9	H	6.972	1.042	-3.866	72	H	10.469	-3.769	-2.614
10	H	5.804	-0.108	-4.515	73	C	8.683	-3.673	-0.175
11	H	9.698	-1.324	-3.395	74	H	8.843	-4.01	0.839
12	H	8.948	-0.134	-2.332	75	H	8.446	-4.519	-0.803
13	H	9.321	0.287	-4.003	76	H	7.863	-2.97	-0.195
14	H	8.212	-1.849	-5.633	77	C	12.556	-1.436	-0.952
15	H	6.767	-2.576	-4.933	78	O	13.603	-2.071	-0.822
16	H	8.354	-2.95	-4.264	79	O	12.16	-0.75	-2.048
17	N	5.852	-1.188	-0.646	80	C	13.025	-0.818	-3.17
18	H	5.648	-2.141	-0.745	81	H	13.383	-1.828	-3.294
19	C	5.618	-0.559	0.647	82	H	13.867	-0.161	-3.022
20	H	5.262	0.444	0.468	83	H	12.505	-0.52	-4.072
21	C	4.554	-1.333	1.425					
22	H	3.89	-0.625	1.897					
23	H	5.039	-1.92	2.19					
24	N	3.766	-2.221	0.626					
25	C	2.762	-1.542	-0.189					
26	H	1.872	-1.377	0.398					
27	H	2.522	-2.154	-1.047					
28	H	3.15	-0.591	-0.52					
29	C	3.141	-3.299	1.389					
30	H	3.905	-3.916	1.835					
31	H	2.531	-3.899	0.727					
32	H	2.524	-2.879	2.168					
33	C	6.91	-0.488	1.457					
34	O	7.747	-1.388	1.392					
35	N	7.099	0.591	2.237					
36	C	8.294	0.778	3.056					
37	H	8.538	-0.115	3.61					
38	C	7.905	1.905	4.03					
39	H	8.509	2.778	3.83					
40	H	8.071	1.576	5.045					
41	C	6.454	2.181	3.781					
42	H	6.263	3.241	3.868					
43	H	5.85	1.632	4.487					
44	C	6.173	1.715	2.382					
45	H	6.395	2.494	1.669					
46	H	5.149	1.391	2.286					
47	C	9.489	1.193	2.211					
48	O	10.631	0.863	2.532					
49	N	9.236	2.117	1.291					
50	H	8.322	2.466	1.225					
51	C	9.98	2.107	0.003					
52	C	10.162	3.422	-0.747					
53	C	9.205	2.378	-1.28					
54	H	9.629	4.318	-0.463					
55	H	10.952	3.58	-1.464					
56	H	9.539	2.006	-2.238					
57	H	8.203	2.778	-1.281					
58	C	11.115	1.133	-0.147					
59	O	12.253	1.474	0.175					
60	N	10.682	-0.121	-0.057					
61	H	9.731	-0.312	-0.205					
62	C	11.594	-1.227	0.213					
63	H	12.165	-0.977	1.095					

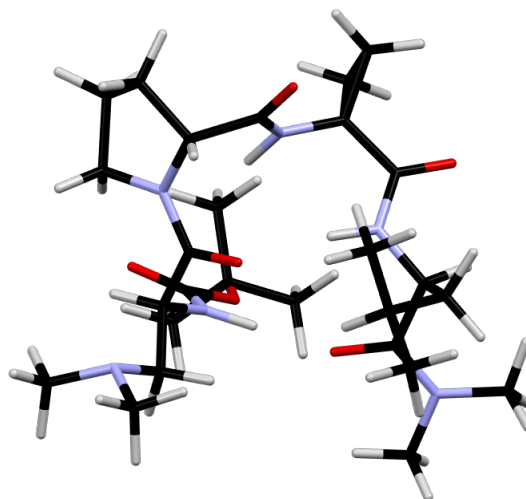
*Average of the 10 lowest-energy scored structures generated by CNS.



F. DFT-Optimization of the CNS Output for Peptides 3 and 4I

Table S5: Optimized Coordinates of Peptide 3 using B3LYP/6-31G(d,p)

Tag	Symbol	X	Y	Z	Tag	Symbol	X	Y	Z
1	O	3.543073	-1.293094	-0.646879	62	C	-3.07787	-0.689807	0.436976
2	C	2.357681	-1.595117	-0.766759	63	H	-3.535358	-1.385389	1.142712
3	O	1.808487	-2.788027	-0.438325	64	C	-4.137868	0.377649	0.054945
4	C	2.619676	-3.875842	0.132909	65	H	-4.570759	0.7517	0.99016
5	C	3.695996	-4.31157	-0.866473	66	H	-4.949994	-0.140264	-0.468976
6	C	3.21395	-3.439091	1.475815	67	C	-3.634585	1.567515	-0.80678
7	C	1.586357	-4.986944	0.334369	68	H	-2.697272	1.275008	-1.29428
8	H	3.23865	-4.574693	-1.825366	69	C	-4.650207	1.906155	-1.909277
9	H	4.214653	-5.19623	-0.483595	70	H	-4.306252	2.750065	-2.51715
10	H	4.425174	-3.517783	-1.029029	71	H	-5.620862	2.182946	-1.478942
11	H	3.717806	-4.288076	1.948509	72	H	-4.813918	1.054964	-2.580059
12	H	2.420266	-3.099452	2.149189	73	C	-3.345702	2.808044	0.053373
13	H	3.935829	-2.633428	1.340765	74	H	-2.92902	3.61624	-0.556807
14	H	2.065942	-5.87183	0.762606	75	H	-2.633175	2.59831	0.854369
15	H	1.131274	-5.266564	-0.62	76	H	-4.269769	3.178754	0.515292
16	H	0.793506	-4.658852	1.012419	77	C	-2.575769	-1.452742	-0.804606
17	N	1.393016	-0.768313	-1.255489	78	O	-1.488465	-1.159663	-1.318267
18	H	0.419664	-1.072123	-1.24337	79	N	-3.377233	-2.415965	-1.342822
19	C	1.687983	0.587378	-1.699948	80	C	-2.961095	-3.083102	-2.573046
20	H	2.773484	0.676225	-1.729595	81	C	-4.651045	-2.879099	-0.806303
21	C	1.09403	0.860169	-3.089088	82	H	-3.733366	-2.967976	-3.342322
22	H	0.006689	0.806949	-2.997736	83	H	-2.030747	-2.638412	-2.917797
23	H	1.412024	0.059022	-3.778392	84	H	-2.809687	-4.153777	-2.392557
24	N	1.47185	2.194283	-3.55564	85	H	-4.630675	-3.97039	-0.708979
25	C	2.772211	2.207061	-4.215464	86	H	-4.855993	-2.457551	0.173872
26	H	2.782087	1.634149	-5.162358	87	H	-5.475059	-2.612945	-1.479622
27	H	3.538796	1.780903	-3.56151					
28	H	3.063008	3.238091	-4.440585					
29	C	0.445684	2.810811	-4.388443					
30	H	0.261229	2.26761	-5.334674					
31	H	0.747507	3.831751	-4.644352					
32	H	-0.493884	2.863911	-3.831938					
33	C	1.073686	1.568498	-0.684456					
34	O	-0.14225	1.795162	-0.686469					
35	N	1.869855	2.080705	0.292021					
36	C	1.27032	2.982321	1.289541					
37	H	0.681256	3.756148	0.792018					
38	C	2.494727	3.572786	2.027051					
39	H	2.272064	3.793102	3.073133					
40	H	2.785972	4.510869	1.543922					
41	C	3.592171	2.513315	1.834266					
42	H	3.465691	1.697889	2.554774					
43	H	4.60129	2.914076	1.956087					
44	C	3.342742	1.997793	0.41159					
45	H	3.692651	0.975785	0.253668					
46	H	3.818891	2.651622	-0.330752					
47	C	0.274978	2.2932	2.242777					
48	O	-0.519903	2.967812	2.885315					
49	N	0.382094	0.932794	2.341785					
50	H	1.038691	0.475803	1.723809					
51	C	-0.494289	0.107949	3.121107					
52	C	-0.600351	0.388925	4.606347					
53	C	0.15891	-0.812732	4.147492					
54	H	-0.054433	1.251989	4.966777					
55	H	-1.580845	0.231462	5.040029					
56	H	-0.302947	-1.785208	4.272931					
57	H	1.243253	-0.788416	4.191314					
58	C	-1.73917	-0.45159	2.464323					
59	O	-2.504018	-1.173537	3.111593					
60	N	-1.943221	-0.138176	1.157245					
61	H	-1.282153	0.435898	0.643504					

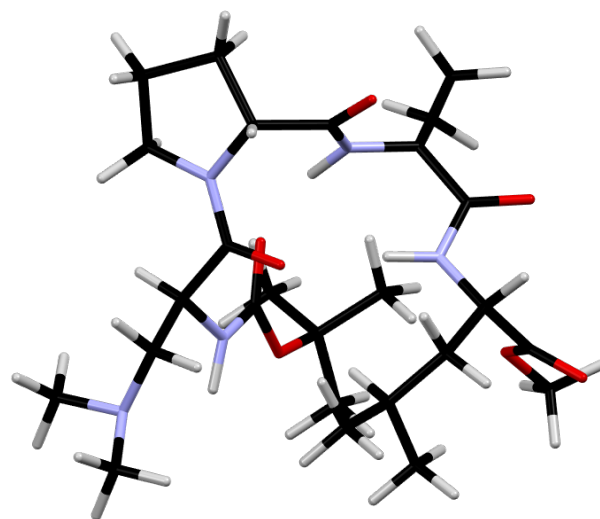


Summary

Calculation Type = FREQ
 Calculation Method = RB3LYP
 Basis Set = 6-31G(d,p)
 Charge = 0
 Spin = Singlet
 E(RB3LYP) = -1837.78766095 a.u.
 RMS Gradient Norm = 0.00000318 a.u.
 Imaginary Freq = 0
 Dipole Moment = 5.2735 Debye
 Point Group = C1

Table S6: Optimized Coordinates of Peptide **4l** using B3LYP/6-31G(d,p)

Tag	Symbol	X	Y	Z	Tag	Symbol	X	Y	Z
1	O	1.080039	0.290934	1.961257	64	C	-2.073017	-0.850499	-2.926696
2	C	1.098664	-0.91055	1.684324	65	H	-1.493098	-0.11487	-3.496244
3	O	0.452624	-1.888753	2.342655	66	H	-2.8074	-1.274943	-3.621486
4	C	-0.41204	-1.608533	3.507354	67	C	-1.117541	-1.966792	-2.450361
5	C	0.442969	-1.070898	4.657969	68	H	-0.487865	-1.570091	-1.645381
6	C	-1.53902	-0.649914	3.115741	69	C	-1.844899	-3.216165	-1.92973
7	C	-0.968511	-2.994703	3.839985	70	H	-2.534255	-3.616349	-2.682946
8	H	-0.179112	-0.94416	5.549542	71	H	-2.414973	-3.011769	-1.021112
9	H	0.881704	-0.106413	4.39922	72	H	-1.122773	-4.004459	-1.68887
10	H	1.245118	-1.774906	4.900307	73	C	-0.182992	-2.342712	-3.611593
11	H	-2.024771	-0.98264	2.194352	74	H	-0.751924	-2.709077	-4.47541
12	H	-1.16518	0.361458	2.961116	75	H	0.510303	-3.138028	-3.314793
13	H	-2.287702	-0.627275	3.914132	76	H	0.409117	-1.481506	-3.937378
14	H	-1.61774	-2.934598	4.718145	77	C	-3.920999	-0.889307	-1.158335
15	H	-0.157606	-3.696236	4.05595	78	O	-4.919807	-1.282306	-1.725609
16	H	-1.552033	-3.387438	3.002457	79	O	-3.637376	-1.17914	0.126417
17	N	1.793402	-1.427558	0.637598	80	C	-4.658019	-1.923404	0.816874
18	H	1.903133	-2.432215	0.556198	81	H	-4.807472	-2.898764	0.347754
19	C	2.766459	-0.636348	-0.092953	82	H	-5.60059	-1.372533	0.80543
20	H	3.547898	-0.292829	0.590885	83	H	-4.296319	-2.041117	1.837611
21	C	3.373629	-1.527429	-1.195399					
22	H	4.208886	-0.981715	-1.671545					
23	H	2.60066	-1.674099	-1.954294					
24	N	3.774429	-2.838491	-0.688053					
25	C	4.965759	-2.77774	0.157087					
26	H	5.853	-2.39801	-0.381886					
27	H	5.197638	-3.778661	0.531573					
28	H	4.7897	-2.133387	1.022765					
29	C	3.951248	-3.800489	-1.775089					
30	H	3.030074	-3.873952	-2.359751					
31	H	4.169786	-4.787112	-1.356102					
32	H	4.774443	-3.530564	-2.460646					
33	C	2.074903	0.570696	-0.759764					
34	O	1.134449	0.389815	-1.542433					
35	N	2.523308	1.813334	-0.464553					
36	C	1.871156	2.990513	-1.067166					
37	H	2.033045	2.98888	-2.149418					
38	C	2.585541	4.184221	-0.392161					
39	H	2.037726	4.474322	0.511116					
40	H	2.627347	5.051559	-1.052778					
41	C	3.963272	3.626327	-0.014357					
42	H	4.451226	4.192014	0.783057					
43	H	4.627346	3.627795	-0.885367					
44	C	3.659658	2.182845	0.405094					
45	H	3.363473	2.114056	1.458588					
46	H	4.514806	1.523971	0.242066					
47	C	0.351233	3.094598	-0.884355					
48	O	-0.295366	3.761429	-1.683725					
49	N	-0.184776	2.518707	0.232992					
50	H	0.368807	1.873145	0.791844					
51	C	-1.590771	2.618876	0.508341					
52	C	-2.140908	3.986215	0.85994					
53	C	-1.996791	2.95855	1.935817					
54	H	-1.432288	4.805425	0.824731					
55	H	-3.137188	4.199227	0.491405					
56	H	-2.895669	2.474922	2.301656					
57	H	-1.190867	3.066059	2.655046					
58	C	-2.541041	1.713341	-0.245183					
59	O	-3.761885	1.867084	-0.156548					
60	N	-1.99645	0.719052	-0.99631					
61	H	-0.991338	0.663957	-1.127354					
62	C	-2.867953	-0.041353	-1.877758					
63	H	-3.487817	0.669033	-2.437763					



Summary

Calculation Type = FREQ
 Calculation Method = RB3LYP
 Basis Set = 6-31G(d,p)
 Charge = 0
 Spin = Singlet
 E(RB3LYP) = -1818.33861237 a.u.
 RMS Gradient Norm = 0.00000346 a.u.
 Imaginary Freq = 0
 Dipole Moment = 13.3420 Debye
 Point Group = C1

VI. Crystallographic Information

A. Experimental

Low-temperature diffraction data (ω -scans) were collected on a Rigaku MicroMax-007HF diffractometer coupled to a Saturn994+ CCD detector with Cu K α ($\lambda = 1.54178 \text{ \AA}$) for the structures of **3(c)** and **4I**. The diffraction images were processed and scaled using the Rigaku CrystalClear software.¹³ The structure was solved with SHELXT and was refined against F^2 on all data by full-matrix least squares with SHELXL.¹⁴ All non-hydrogen atoms were refined anisotropically. Hydrogen atoms were included in the model at geometrically calculated positions and refined using a riding model. Unless stated otherwise, the isotropic displacement parameters of all hydrogen atoms were fixed to 1.2 times the U value of the atoms to which they are linked (1.5 times for methyl groups). The full numbering scheme of compound **3(c)** and **4I** can be found in Figures S4 and S5, respectively. Full details of the X-ray structure determination are in the CIFs included as Supporting Information. CCDC number 1453125 (**3(c)**) and 1453124 (**4I**) contain the supplementary crystallographic data for this paper. These data can be obtained free of charge from The Cambridge Crystallographic Data Center via http://www.ccdc.cam.ac.uk/data_request/cif.

Data and Refinement Details for 3c

The only exceptions are hydrogen atoms H2, H3 and H5, which are freely refining and a part of refined hydrogen bond interactions.

Data and Refinement Details for 4I

Multiple attempts to collect data at 93 K resulted in streaky reflections. The data reported here were collected at 228 K, which obscured the already difficult to locate hydrogen atoms associated with the heteroatoms. The model reported here uses riding models and geometrically placed hydrogen atoms on heteroatoms. The ester and butyl residues are disordered over two equally occupied positions. The atoms involved are distinguished with the suffix "a" and "b". The atomic displacement parameters are large (due to the relatively high temperature need for data collection). Subsequently, rigid bond restraints were used to aid the refinement.

Table S7: Details of X-Ray Crystal Structures **3(a–c)** and **4I**

Compound	3(a,b)*	3(c)	4I
Data Code	007-15050	007-15126	007-15146
Empirical Formula	C ₂₇ H ₄₉ N ₆ O _{6.5}	C ₂₇ H ₄₈ N ₆ O ₆	C ₂₆ H ₄₄ N ₅ O ₇
Temperature (K)	93(2)	93(2)	228(2)
FW	561.72	552.71	538.66
Crystal System	Monoclinic	Orthorombic	Orthorombic
Space Group	<i>P</i> 2 ₁	<i>P</i> 2 ₁ 2 ₁ 2 ₁	<i>P</i> 2 ₁ 2 ₁ 2 ₁
<i>a</i> (Å)	16.1717(11)	11.7899(8)	11.9360(8)
<i>b</i> (Å)	9.364(6)	15.9908(11)	16.0501(11)
<i>c</i> (Å)	21.5606(15)	16.3363(11)	16.5597(12)
α (deg)	90	90	90
β (deg)	104.7162(2)	90	90
γ (deg)	90	90	90
<i>V</i> (Å ³)	3157.9(4)	3079.9(4)	3172.4(4)
<i>Z</i>	4	4	4
ρ (g/cm ³)	1.181	1.192	1.128
μ (mm ⁻¹)	0.693	0.691	0.676
Absolute Structure Parameter	-0.04(15)	0.01(4)	-0.01(3)
<i>R</i> 1, <i>wR</i> 2 (<i>I</i> > 2 <i>s</i> (<i>I</i>))	0.0651, 0.1665	0.0287, 0.0784	0.0504, 0.1454
<i>R</i> 1, <i>wR</i> 2 (all data)	0.9082, 0.1864	0.0307, 0.0792	0.0534, 0.1513
GOF	1.023	1.060	1.023
Largest Diff. Peak, Hole (e Å ⁻³)	0.760, -0.285	0.274, -0.166	0.280, -0.190

*Data reported in ref. 6 (CSD entry 1412920).

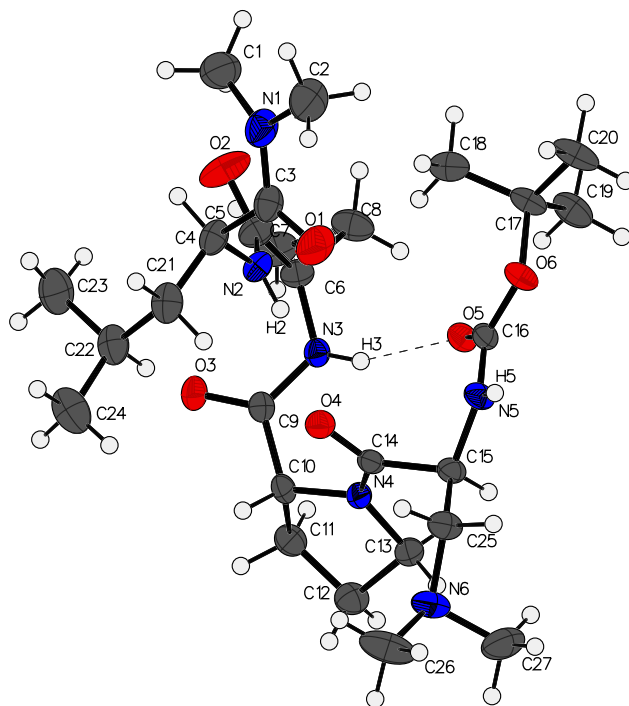


Figure S4: The full numbering scheme of **3(c)** with 50% thermal ellipsoids. The hydrogen atoms are depicted as circles for clarity.

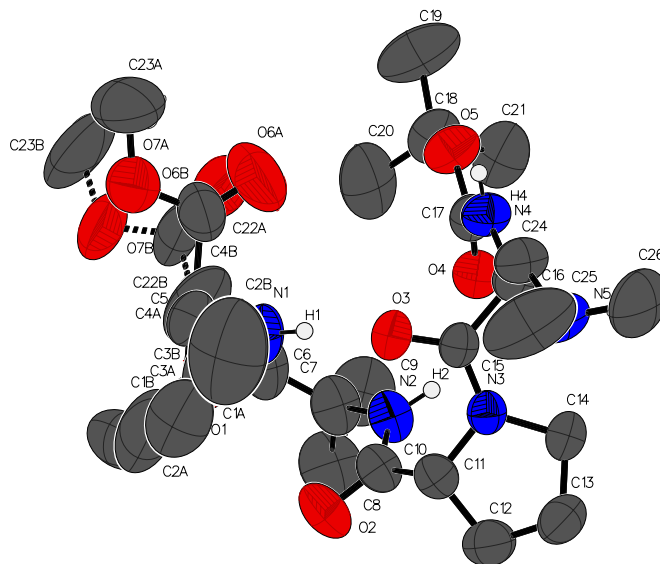


Figure S5: The full numbering scheme of **4I** with 50% thermal ellipsoids. Most of the hydrogen atoms are either not shown or depicted as circles for clarity.

B. Definition of Planes Describing Backbone Bending in Conformers 3(a,b)

To describe the degree of backbone-bending observed in the type II' β -turn conformers of peptide **3**, we measured the angle between two defined planes, which were calculated using the program Mercury (Figure S6).¹⁵ For both conformers **3(a)** and **3(b)**, **Plane 1** was defined by the α -carbons of i , $i+1$, $i+2$, and $i+3$, and **Plane 2** was defined by the α -carbons of i , $i+3$ (*trans*-Me C-atom of the NMe₂-group) $i+4$, and $i-1$ (3° C-atom of the Boc-group).

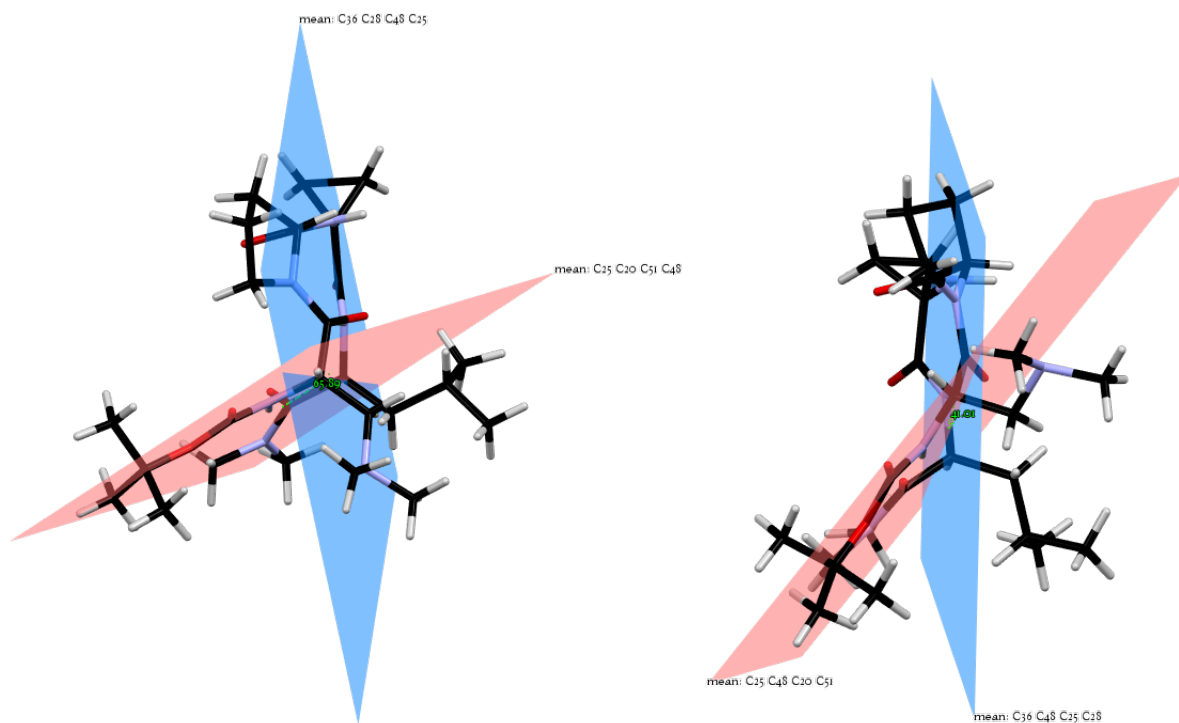


Figure S6: Intersecting planes that describe the backbone bending of conformers **3(a)** (left) and **3(b)** (right). The backbone bend of **3(a)** was measured to be 65.9°, while the bend of **3(b)** was measured to be 41.0°.

VII. References

1. G. R. Fulmer, A. J. M. Miller, N. H. Sherden, H. E. Gottlieb, A. Nudelman, B. M. Stoltz, J. E. Bercaw, and K. I. Goldberg, *Organometallics*, 2010, **29**, 2176.
2. C. A. G. N. Montalbetti and V. Falque, *Tetrahedron*, 2005, **61**, 10827; A. El-Faham, F. Albericio, *Chem. Rev.*, 2011, **111**, 6557.
3. L.-H. Zhang, G. S. Kauffman, J. A. Pesti, and J. Yin, *J. Org. Chem.*, 1997, **62**, 6918.
4. T. Nagase, T. Mizutani, S. Ishikawa, E. Sekino, T. Sasaki, T. Fujimura, T. S. Ito, Y. Mitobe, Y. Miyamoto, R. Yoshimoto, T. Tanaka, A. Ishihara, N. Takenaga, S. Tokita, T. Fukami, and F. Sato, *J. Med. Chem.* 2008, **51**, 4780.
5. I. I. Ponomarev, D. Y. Razorenov, and P. V. Petrovskii, *Russ. Chem. Bull.* 2009, **58**, 2376.
6. M. E. Diener, A. J. Metrano, S. Kusano, and S. J. Miller, *J. Am. Chem. Soc.*, 2015, **137**, 12369.
7. B. A. Borgia, M. Gochin, D. J. Kehrwood, and T. L. James, *Prog. NMR Spectrosc.*, 1990, **22**, 83.
8. S. Macura, B. T. Farmer, II, and L. R. Brown, *J. Mag. Res.*, 1986, **70**, 493.
9. A. T. Brunger, P. D. Adams, G. M. Clore, P. Gros, R. W. Kunstleve-Grosse, J. Kuszewski, N. Nilges, N. S. Pannu, R. J. Read, L. M. Rice, T. Simonson, and G. L. Warren, *Acta Cryst.*, 1998, **54**, 905; A. T. Brunger, *Nature Protocols*, 2007, **2**, 272.
10. All computational work was supported by the facilities and staff of Yale University Faculty of Arts and Sciences High Performance Computing Center, and by the National Science Foundation under grant #CNS 08-21132 that partially funded acquisition of the facilities.
11. Gaussian 09, Revision **D.01**, M. J. Frisch, G. W. Trucks, H. B. Schlegel, G. E. Scuseria, M. A. Robb, J. R. Cheeseman, G. Scalmani, V. Barone, B. Mennucci, G. A. Petersson, H. Nakatsuji, M. Caricato, X. Li, H. P. Hratchian, A. F. Izmaylov, J. Bloino, G. Zheng, J. L. Sonnenberg, M. Hada, M. Ehara, K. Toyota, R. Fukuda, J. Hasegawa, M. Ishida, T. Nakajima, Y. Honda, O. Kitao, H. Nakai, T. Vreven, J. A. Montgomery, Jr., J. E. Peralta, F. Ogliaro, M. Bearpark, J. J. Heyd, E. Brothers, K. N. Kudin, V. N. Staroverov, R. Kobayashi, J. Normand, K. Raghavachari, A. Rendell, J. C. Burant, S. S. Iyengar, J. Tomasi, M. Cossi, N. Rega, J. M. Millam, M. Klene, J. E. Knox, J. B. Cross, V. Bakken, C. Adamo, J. Jaramillo, R. Gomperts, R. E. Stratmann, O. Yazyev, A. J. Austin, R. Cammi, C. Pomelli, J. W. Ochterski, R. L. Martin, K. Morokuma, V. G. Zakrzewski, G. A. Voth, P. Salvador, J. J. Dannenberg, S. Dapprich, A. D. Daniels, Ö. Farkas, J. B. Foresman, J. V. Ortiz, J. Cioslowski, and D. J. Fox, Gaussian, Inc., Wallingford CT, 2009.
12. J. Tomasi, B. Mennucci, and R. Cammi, *Chem. Rev.*, 2005, **105**, 2999.
13. CrystalClear and CrystalStructure; Rigaku/MS: The Woodlands, TX, 2005.
14. G. M. Sheldrick, *Acta Cryst.*, 2008, **A64**, 112.
15. Mercury CSD, **2.0**, C. F. Macrae, I. J. Bruno, J. A. Chisholm, P. R. Edgington, P. McCabe, E. Pidcock, L. Rodriguez-Monge, R. Taylor, J. van de Streek and P. A. Wood, *J. Appl. Cryst.*, 2008, **41**, 466.